AAE

AERONAUTICAL AND ASTRONAUTICAL ENGINEERING DEPARTMENT

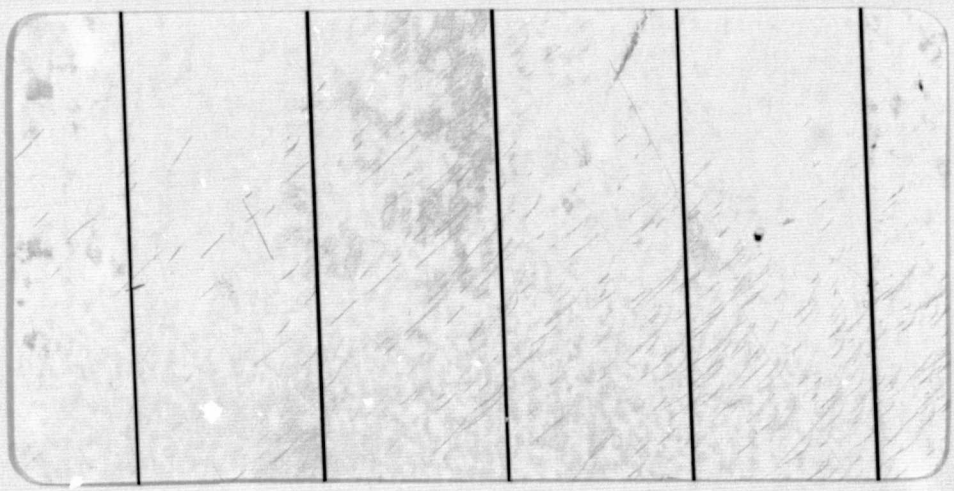

ENGINEERING EXPERIMENT STATION, COLLEGE OF ENGINEERING, UNIVERSITY OF ILLINOIS, URBANA

Aeronautical and Astronautical Engineering Department
University of Illinois Urbana, Illinois

Technical Report AAE 75-5
UILU-Eng 75 0505

NASA Grant NGR 14-005-144
Allen I. Ormsbee, Principal Investigator

DESIGN OF HIGH LIFT AIRFOILS WITH A STRATFORD DISTRIBUTION BY THE EPPLER METHOD

by

William G. Thomson

University of Illinois

Urbana, Illinois

June 1975

TABLE OF CONTENTS

I. INTRODUCTION

High lift airfoils have been the subject of on-going study at the University of Illinois [1,2,3,4,5] for several years. The major part of the present study has been concentrated on airfoils having a Stratford [3,6] pressure distribution, which has zero skin friction in the pressure recovery area. This pressure recovery represents an approximation to maximum pressure recovery without separation.

These airfoils are designed with non-zero velocity at the trailing edge. This non-zero trailing edge velocity is unavoidable, as the zero skin friction velocity approaches a zero velocity tangentially, and it would require an airfoil with an infinitely long chord to have a stagnation point at the trailing edge if a Stratford distribution was used. Chen [3] determined the optimum relationship between the maximum velocity on the upper surface (the "rooftop" velocity) and the trailing edge velocity, and this relationship has been used since then in the design of high lift airfoils at the University of Illinois. However, this relationship does not specify the magnitude of either the rooftop velocity or the trailing edge velocity, but only specifies the ratio between the two velocities. Therefore, as the trailing edge velocity increases, the lift increases (since the rooftop velocity goes up), and the maximum lift possible is limited only by the fact that, as the trailing edge velocity increases, the angle of the trailing edge increases, distorting the shape of the trailing edge.

The Eppler [7,8] program is an inverse conformal mapping technique, where the x and y coordinates of the airfoil are developed from a given velocity distribution. Unfortunately, the velocity distribution is

given in terms of the circle plane, and the transformation from the circle plane to the airfoil is not known until the problem is solved, so the Stratford distribution cannot be used as a direct input to the Eppler program. The problem is further complicated by the fact that the roof-top velocity is not known until the problem is solved, so the desired velocity distribution (the Stratford distribution) is not known until after the shape of the airfoil has been determined by the Eppler program. Therefore, the solution of the problem involves visually comparing the output of the Eppler program with a Stratford distribution, and then guessing the modifications to the input of the Eppler program to get the desired output. With experience in determining the changes required in the input to the Eppler program to yield the desired changes in the output, the number of iterations required to determine the correct airfoil decreases to a reasonable amount.

II. THE EPPLER METHOD

The method developed by Eppler [7,8] is an inverse conformal mapping technique that determines the x and y coordinates from a given velocity distribution. The two planes involved are shown in figure 1. The ζ plane shows the flow about a circular cylinder, while the z plane represents the flow about the airfoil. The velocity in the z plane is given in terms of coordinates determined in the ζ plane. z and ζ are defined as:

$$z = x + iy \tag{1}$$

$$\zeta = \xi + i\eta = re^{i\phi} \tag{2}$$

The flow in the ζ plane is such that the rear stagnation point falls on the real axis at $\zeta = 1$.

There exists a transformation of the ζ plane to the z plane such that the z plane represents parallel flow about a closed airfoil at an angle of attack α. Since $\zeta = 1$ represents a stagnation point, the Kutta condition requires that this must transform to the trailing edge of the airfoil. As this is to be an infinite parallel flow, $z(\infty) = \infty$ and $(\frac{dz}{d\zeta})_\infty$ must be real. The general function that satisfies these requirements is

$$(\zeta) = \beta_1\zeta + \sum_{\nu=0}^{\infty} \beta_{-\nu}\zeta^{-\nu} \tag{3}$$

where β_1 is real, but not equal to zero.

The complex potential in the ζ plane can be represented as

$$F(\zeta) = \phi + i\Psi = C(e^{-i\alpha}\zeta + \frac{e^{i\alpha}}{\zeta}) - \frac{\Gamma}{2\pi i} \ln \zeta \tag{4}$$

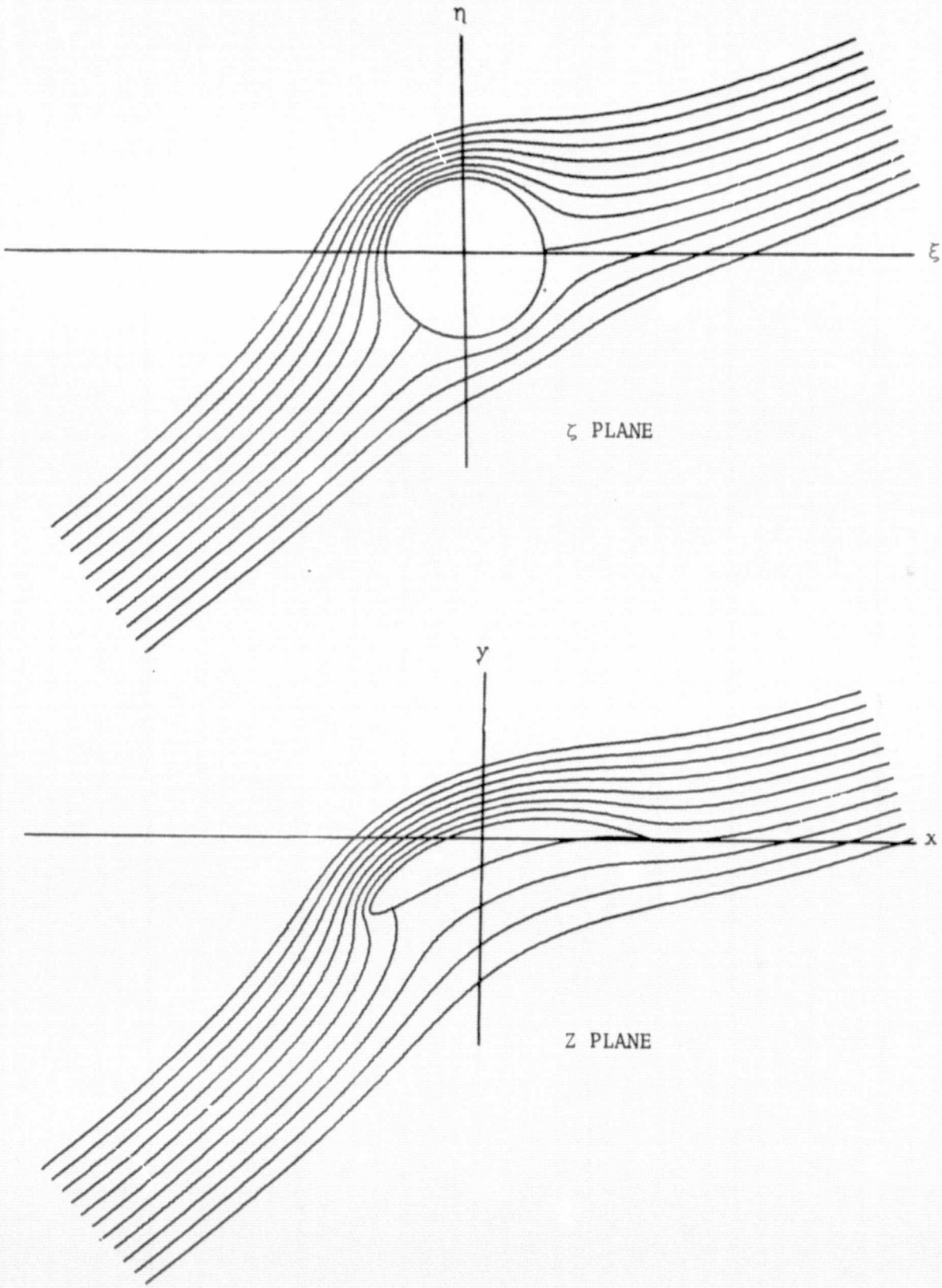

Figure 1. The complex mapping planes

where Γ is given by

$$\Gamma = 4\pi C \sin\alpha \tag{5}$$

The complex velocity in the z plane is given by

$$Ve^{-i\theta} = \frac{dF}{dz} = \frac{dF/d\zeta}{dz/d\zeta} \tag{6}$$

The inverse of this will be used, or

$$\frac{dz}{dF} = \frac{dz/d\zeta}{dF/d\zeta} \tag{7}$$

In order to prevent an undesirable root, this can be written as

$$\ln \frac{dz}{dF} = \ln \frac{dz}{d\zeta} - \ln \frac{dF}{d\zeta} \tag{8}$$

The velocity vector in the z plane can be introduced as $\overline{V} = Ve^{i\theta}$. Then

$$\frac{dF}{dz} = Ve^{-i\theta} \tag{9}$$

Therefore,

$$\ln \frac{dz}{dF} = - \ln V + i\theta \tag{10}$$

The real part of $\ln \frac{dz}{dF}$ is then $-\ln V$. Outside the boundary of the unit circle, $\ln \frac{dz}{dF}$ is regular, and can be calculated when the real part is known on the boundary. Since $F(\zeta)$ is also known (eq.(4)), equation (8) can be solved for $\frac{dz}{d\zeta}$. $z(\zeta)$ then can be found by integration. $z(\zeta)$ must be of the form of equation (3) to match the boundary conditions. Therefore, the problem is to find an equation for $\ln \frac{dz}{dF}$ which results in a satisfactory $\frac{dz}{d\zeta}$.

From equations (4) and (5)

$$\frac{dF}{d\zeta} = -e^{i\alpha} C \left(\frac{1}{\zeta} - 1\right) \left(\frac{1}{\zeta} + e^{-2i\alpha}\right) \tag{11}$$

In light of the singularities involved at the stagnation points, $\ln \frac{dz}{dF}$ can be represented by

$$\ln\frac{dz}{dF} = -\ln C - \ln \left[e^{i\alpha} \left(\frac{1}{\zeta} + e^{-2i\alpha}\right)\right] + \sum_{m=0}^{\infty} (a_m + ib_m)\, \zeta^{-m} \tag{12}$$

Using this equation and equations (8) and (11),

$$\ln \frac{dz}{d\zeta} = \ln \left(1 - \frac{1}{\zeta}\right) + \sum_{m=0}^{\infty} (a_m + ib_m)\, \zeta^{-m} \tag{13}$$

This results in

$$\frac{dz}{d\zeta} = \left(1 - \frac{1}{\zeta}\right) e^{\sum_{m=0}^{\infty} (a_m + ib_m)\, \zeta^{-m}} \tag{14}$$

Expanding this yields

$$\frac{dz}{d\zeta} = \left(1 - \frac{1}{\zeta}\right) e^{a_o + ib_o} e^{(a_1 + ib_1)\zeta^{-1}} e^{(a_2 + ib_2)\zeta^{-2}} \cdots\cdots \tag{15}$$

$z(\zeta)$ must be of the form of equation (3), so $\frac{dz}{d\zeta}$ must be of the form

$$\frac{dz}{d\zeta} = \beta_1 + \sum_{\nu=1}^{\infty} -\nu\beta_{-\nu}\zeta^{-\nu-1} \tag{16}$$

If we let $A_n = a_n + ib_n$, equation (15) can be further expanded to

$$\frac{dz}{d\zeta} = \left(1 - \frac{1}{\zeta}\right)\left(1 + A_o + \frac{A_o^2}{2!} + \frac{A_o^3}{3!} + \ldots\right)\left(1 + \frac{A_1}{\zeta} + \frac{A_1^2}{2!\zeta^2} + \frac{A_1^3}{3!\zeta^3} + \ldots\right)\left(1 + \frac{A_2}{\zeta^2} + \frac{A_2^2}{2\zeta^4} + \ldots\right)\ldots \tag{17}$$

Comparing equations (16) and (17) yields

$$\beta_1 = 1 + A_o + \frac{A_o^2}{2!} + \frac{A_o^3}{3!} + \ldots = e^{A_o} \tag{18}$$

Since β_1 is real, A_o is also real. At infinity, we want $\frac{dz}{d\zeta} = 1$, indicating that the flow at infinity in the circle plane is in the same direction as the flow at infinity in the airfoil plane. From equation (16), $\frac{dz}{d\zeta} = \beta_1$ at infinity. Therefore,

$$\beta_1 = e^{A_o} = 1 \tag{19}$$

Because of this, $A_o = 0$.

Comparing the $\frac{1}{\zeta}$ term yields

$$-\frac{\beta_1}{\zeta} + \frac{A_1 \beta_1}{\zeta} = 0 \tag{20}$$

So $a_1 = 1$, $b_1 = 0$.

At infinity, we can arbitrarily set the velocity equal to unity. From equation (12), in the limit as $\zeta \to \infty$, $\frac{dF}{dz} = Ce^{-i\alpha}$. Therefore, $C=1$ and $\ln C=0$.

The problem that remains is to define the a_m and b_m that have not yet been defined such that, along the surface of the airfoil, the velocity assumes the prescribed values.

Along the surface of the circle plane, $\zeta = e^{i\phi}$. Using this, equation (12) results in

$$\ln \frac{dz}{dF} = -\ln \left[e^{i\alpha} \left(e^{i\phi} + e^{2i\alpha}\right)\right] + \sum_{m=0}^{\infty} (a_m + ib_m)\, e^{-im\phi} \tag{21}$$

If we use the substitutions

$$P(\phi) = \sum_{m=0}^{\infty} (a_m \cos m\phi + b_m \sin m\phi) \tag{22}$$

$$Q(\phi) = \sum_{m=0}^{\infty} (-a_m \sin m\phi + b_m \cos m\phi) \tag{23}$$

equation (21) can be written as

$$\ln \frac{dz}{dF} - \ln[e^{i\phi/2}(e^{i(\alpha + \phi/2)} + e^{-i(\alpha + \phi/2)})] + P(\phi) + iQ(\phi) \tag{24}$$

This can be written as

$$-\ln V(\phi) + i\theta(\phi) = -\ln 2\left|\cos (\phi/2-\alpha)\right| + P(\phi) + i\left[\frac{\phi}{2} + Q(\phi) - \{\{\pi\}\}\right] \tag{25}$$

where $\{\{\pi\}\}$ is given as

$$\{\{\pi\}\} = \begin{matrix} 0 & (0 \leq \phi < \pi + 2\alpha) \\ \pi & (\pi + 2\alpha < \phi \leq 2\pi) \end{matrix} \tag{26}$$

The $\{\{\pi\}\}$ term is necessary due to the shift in the direction of the velocity at the stagnation point.

The real part of equation (25) can be rearranged into the form

$$P(\phi) = \ln 2\left|\cos \left(\frac{\phi}{2} - \alpha\right)\right| - \ln V(\phi) \tag{27}$$

Through harmonic analysis, the a_m's and b_m's can be determined from equation (27). However, we must have $a_o = 0$, $a_1 = 1$, and $b_1 = 0$, due to equations (19) and (20). Therefore,

$$\int_o^{2\pi} P(\phi)\, d\phi = 0 \tag{28}$$

$$\int_o^{2\pi} P(\phi) \cos\phi\, d\phi = \pi \tag{29}$$

$$\int_o^{2\pi} P(\phi) \sin\phi\, d\phi = 0 \tag{30}$$

The velocity distribution we specify must meet these requirements.

By integrating equation (14), the transformation

$$z(\zeta) = \int (1-1/\zeta)\, e^{\sum_{m=0}^{\infty} (a_m + ib_m)\, \zeta^{-m}}\, d\zeta \qquad (31)$$

can be derived. This yields the flow for the entire z plane. If $\zeta = e^{i\phi}$ is entered into this transformation, the resulting $z = x + iy$ will yield the profile of the airfoil. The results are

$$x(\phi) = \int -4 \sin\frac{\phi}{2} \left|\cos\left(\frac{\phi}{2} - \alpha\right)\right| \frac{1}{V(\phi)} \cos\left(\frac{\phi}{2} + Q(\phi)\right) d\phi \qquad (32)$$

$$y(\phi) = \int -4 \sin\frac{\phi}{2} \left|\cos\left(\frac{\phi}{2} - \alpha\right)\right| \frac{1}{V(\phi)} \sin\left(\frac{\phi}{2} + Q(\phi)\right) d\phi \qquad (33)$$

The only quantity remaining to be defined, then, is $Q(\phi)$. However, $Q(\phi)$ is a conjugate harmonic function of $P(\phi)$, and can be derived from the formula

$$Q(\phi) = \frac{1}{2\pi} \int_0^{2\pi} P(\sigma) \cot\left(\frac{\sigma - \phi}{2}\right) d\sigma \qquad (34)$$

Given a velocity distribution that yields a $P(\phi)$ such that equations (28) through (30) are satisfied, and an angle of attack, the x and y coordinates of the desired airfoil can be generated using equations (32) and (33). The angle of attack, α, need not be held constant, but can be a function of ϕ. Thus, the upper surface can be designed at a different (higher for reasonable airfoils) angle of attack than the lower surface, or even different portions of the upper (or lower) surface can be designed at different angles of attack.

The profile of the airfoil is determined by a_m and b_m. Therefore, for a fixed profile, a_m and b_m are fixed. Altering the angle of attack

will not alter the airfoil profile, and, therefore, will not alter a_m or b_m. This means that $P(\phi)$ is independent of the angle of attack. Equation (27) can, then, be written in the form of

$$P(\phi) = \ln 2\left|\cos\left(\frac{\phi}{2} - \alpha^*(\phi)\right)\right| - \ln V^*(\phi) \tag{35}$$

where $V^*(\phi)$ is the specified velocity at the point on the airfoil corresponding to ϕ, and $\alpha^*(\phi)$ is the corresponding angle of attack. At any angle of attack, α, then, the velocity can be given as

$$V(\phi,\alpha) = \frac{\cos\ (\phi/2-\alpha)}{\cos\ (\phi/2-\alpha^*(\phi))}\ V^*(\phi) \tag{36}$$

The circle plane can be divided into I_a segments, as in figure (2), where $\phi_0 = 0<\phi_1<\phi_2<\ldots.\phi_{I_L}\ldots<\phi_{I_a}$. ϕ_{I_L} indicates the stagnation point. The angle of attack specification takes the form

$$\alpha^*(\phi) = \alpha_i = \text{constant for } \phi_{i-1}<\phi\leq\phi_i \tag{37}$$

and the velocity takes the form

$$V^*(\phi) = V_i W_i(\phi) \tag{37}$$

where V_i is a constant for $\phi_{i-1}<\phi\leq\phi_i$ and $W(\phi)$ is given as

$$W(\phi) = \left[1 + K\left\{\left\{\frac{\cos\phi - \cos\phi_\omega}{1 + \cos\phi_\omega}\right\}\right\}\right]^{-\mu}\left[1 - 0.36\left\{\left\{\frac{\cos\phi - \cos\phi_s}{1 - \cos\phi_s}\right\}\right\}^2\right]^{K_H} \tag{39}$$

on the upper surface. On the lower surface, the velocity distribution is similar, but different values of K_H, μ, ϕ_w, and ϕ_s are used, indicated by $\overline{K}_H$, $\overline{\mu}$, $\overline{\phi}_w$, and $\overline{\phi}_s$, respectively. The terms in the double brackets of equation (38) are defined by

$$\{\{f(\phi)\}\} = \begin{cases} f(\phi) & (f(\phi) > 0) \\ 0 & (f(\phi) \leq 0) \end{cases} \tag{40}$$

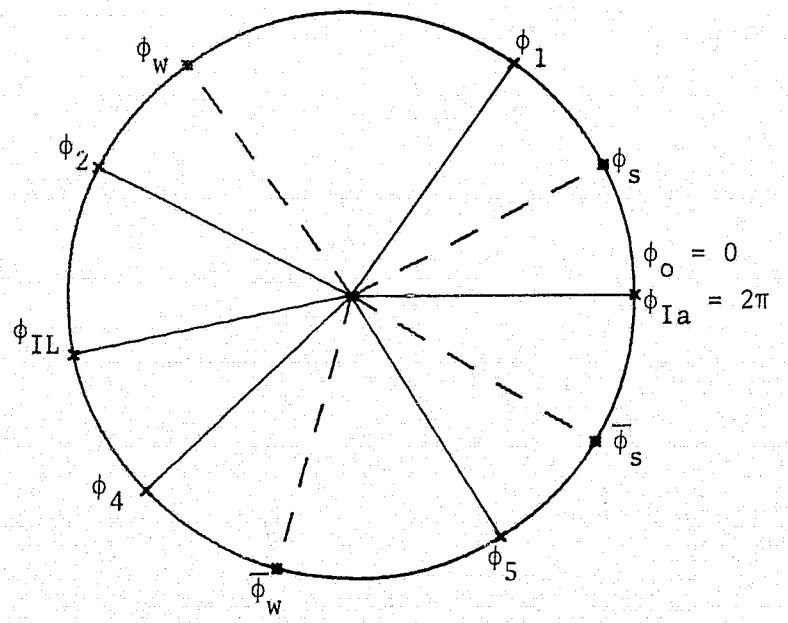

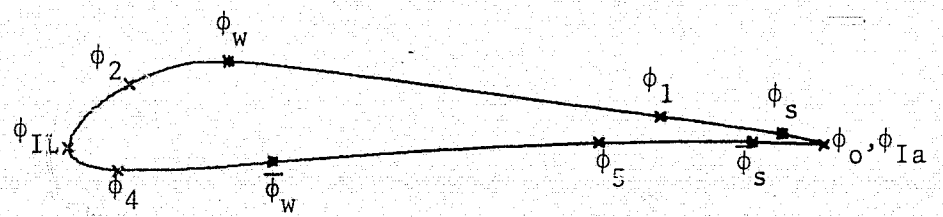

Figure 2. Segementing the profile

Equation (39) can be considered to be of the form

$$W(\phi) = W_w(\phi)\, W_s(\phi)^{K_H} \tag{41}$$

or, on the lower surface

$$W(\phi) - \overline{W}_w(\phi)\, \overline{W}_s(\phi)^{\overline{K}_H} \tag{42}$$

The W_w (or $\overline{W}_w$) term produces the major pressure recovery. This is in the form specified by Wortmann [9], in which the shape parameter is held constant, which delays separation. The W_s (or $\overline{W}_s$) term develops the cusp distribution. It is generally applied to the last 3-5% of the airfoil length. Outside of the range of the specified region, $\phi>\phi_w$ for W_w or $\phi>\phi_s$ for W_s (or $\phi<\overline{\phi}_w$ or $\overline{\phi}_s$ on the lower surface), the value of W_w or W_s is as given by figure (3).

$P(\phi)$ must be continuous over the airfoil, so $P(\phi_i^-) = P(\phi_i^+)$, and $P(0) = P(2\pi)$. Substituting our values for V^* and α^* into equation (27) yields

$$P(\phi) = \ln 2\left|\cos\left(\frac{\phi}{2} - \alpha(\phi)\right)\right| - \ln\left[V_i W_s(\phi) W_s(\phi)\right]^{K_H} \tag{43}$$

Since, at the trailing edge, $P(0) - P(2\pi)$,

$$\ln 2\left|\cos\alpha_1\right| - \ln\left[V_1 W_w(0) W_s(0)^{K_H}\right] = \ln 2\left|\cos\alpha_{I_a}\right| - \ln\left[V_{I_a} \overline{W}_w(2\pi)\, \overline{W}_s(2\pi)\right]^{K_H} \tag{44}$$

At all other segment boundaries, which are generally outside of the cusp region, $W_s = \overline{W}_s = 1$, $P(\phi_i^-) = P(\phi_i^+)$, and therefore

$$\ln 2\left|\cos\left(\frac{\phi_i}{2} - \alpha_i\right)\right| - \ln\left[V_i W_w(\phi_i)\right] = \ln 2\left|\cos\left(\frac{\phi_i}{2} - \alpha_{i+1}\right)\right| - \ln\left[V_{i+1} W_w(\phi_i)\right] \tag{45}$$

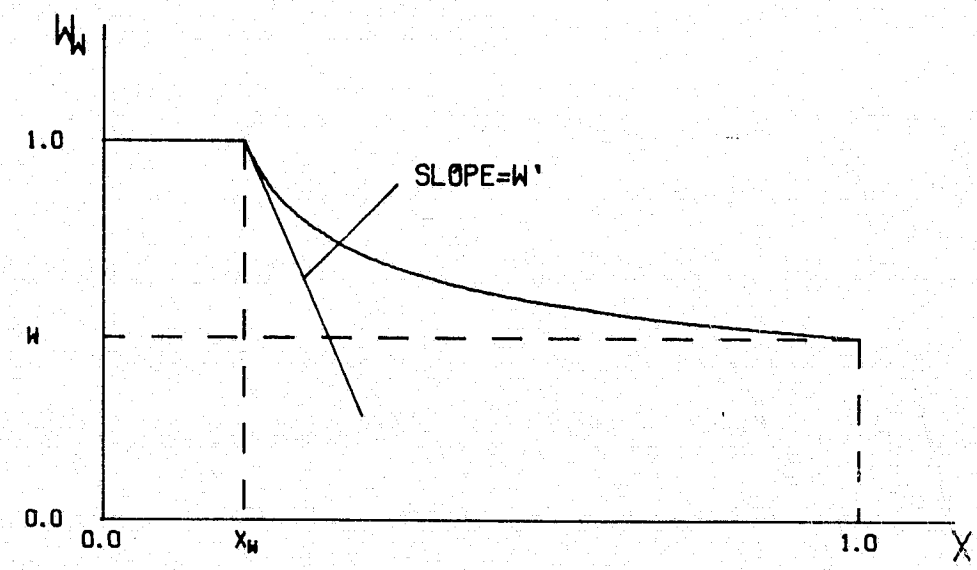

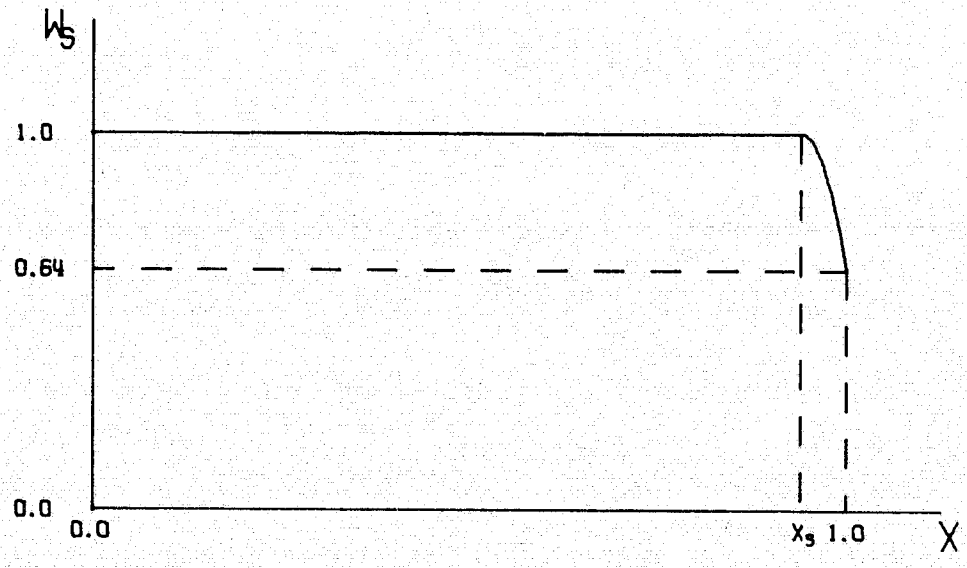

Figure 3. The form of the velocity components.

On the lower surface, W_w is replaced by $\overline{W}_w$ in equation (45).

If, in any segment, $\phi = \pi + 2\alpha_i$, $P(\phi)$ becomes infinite. This is most likely to occur in the segments to either side of the stagnation point, $\phi_{I_L-1} < \phi < \phi_{I_L+1}$, where ϕ_{I_L} indicates the stagnation point. In order to prevent this, we require

$$\alpha_{I_L} > \alpha_{I_L+1} \tag{46}$$

and

$$\pi + 2\alpha_{I_L} > \phi_{I_L} > \pi + 2\alpha_{I_L+1} \tag{47}$$

If all the ϕ_i's and α_i's along with μ, $\overline{\mu}$, ϕ_w, $\overline{\phi}_w$, ϕ_s, and $\overline{\phi}_s$ are given in the problem specification, this leaves only K_H and $\overline{K}_H$ left to be determined. However, with equations (28) through (30) there are three conditions that must be met. Therefore, we need to free one of the quantities listed above. The quantity best suited for this is ϕ_{I_L}, the location of the stagnation point.

If we use equation (43) to define $P(\phi)$, equation (29) becomes

$$\int_0^{2\pi} [\ln\left|\cos\left(\frac{\phi}{2} - \alpha(\phi)\right)\right| - \ln V(\phi) - \ln W_w(\phi) - K_H \ln W_s(\phi) + \ln 2] \cos\phi d\phi = \pi \tag{48}$$

This can be expanded to

$$\sum_{i=1}^{I_L} \int_{\phi_{i-1}}^{\phi_i} [\ln\left|\cos\left(\frac{\phi}{2} - \alpha_i\right)\right| - \ln V_i - \ln W_w - K_H \ln W_s + \ln 2] \cos\phi d\phi$$

$$+ \sum_{i=I_L}^{I_a} \int_{\phi_{i-1}}^{\phi_i} [\ln\left|\cos\left(\frac{\phi}{2} - \alpha_i\right)\right| - \ln V_i - \ln \overline{W}_w - \overline{K}_H \ln \overline{W}_s + \ln 2] \cos\phi d\phi = \pi \tag{49}$$

The integral $\int \cos\phi \ln\left|\cos\frac{\phi}{2} - \alpha_i\right| d\phi$ can be evaluated as

$$\int \cos\phi \ln\left|\cos\frac{\phi}{2} - \alpha_i\right| d\phi = (\sin\phi + \sin 2\alpha_i) \ln\left|\cos\frac{\phi}{2} - \alpha_i\right| + \frac{1}{2}(\phi\cos 2\alpha_i - \sin\phi) + \text{constant} \tag{50}$$

If we denote W_{ci} as

$$W_{ci} = -\int_{\phi_{i-1}}^{\phi_i} \cos\phi \ln W_s(\phi)\, d\phi \tag{51}$$

and introduce the notation

$$\ln(i,j) = \ln\left|\cos\left(\frac{\phi_i}{2} - \alpha_i\right)\right| \tag{52}$$

equation (49) can be written as

$$K_H W_{c1} + \overline{K}_H W_{cI_a} + \sum_{i=1}^{I_a} \sin 2\alpha_i (\ln(i,i) - \ln(i-1,i)) + \frac{1}{2}(\phi_i - \phi_{i-1})\cos 2\alpha_i + \frac{1}{2}(\sin\phi_i - \sin\phi_{i-1}) + \sin\phi_i [\ln(i,i) - \ln V_i] - \sin\phi\,[\ln(i-1,i) - \ln V_i]\} - \int_0^{\phi_w} \cos\phi \ln W_w d\phi - \int_{\phi_w}^{2\pi} \cos\phi \ln \overline{W}_w(\phi)\, d\phi = \pi \tag{53}$$

Due to equation (45), the next to the last term, with i=n, and the last term, with i=n+1 (n=1, I_a-1), cancel each other out. Out of these terms, only the last with i=1 and the next to the last with $i=I_a$ remain. However, since $\phi_o=0$ and $\phi_{I_a} = 2\pi$, $\sin\phi_o = \sin\phi_{I_a} = 0$, these terms also drop out. The third term of the summation also drops out. Therefore, equation (53) can be written as

$$K_H W_{cl} + \overline{K}_H W_{cI_a} + \sum_{i=1}^{I_a} \{\sin 2\alpha_i \ (\ln(i,i) - \ln(i-1,i)) + \frac{1}{2} (\phi_i - \phi_{i-1}) \cos 2\alpha_i\} - \int_o^{\phi_w} \cos\phi \ln W_w \, d\phi - \int_{\phi_w}^{2\pi} \cos\phi \ln \overline{W}_w (\phi) \, d\phi = \pi \quad (54)$$

We now introduce J_c such that

$$J_c = \sum_{i=1}^{I_a} \{\sin 2\alpha_i ((\ln(i,i) - \ln (i-1,i)) + \frac{1}{2} (\phi_i - \phi_{i-1}) \cos 2\alpha_i\} - \int_o^{\phi_w} \cos\phi \ln W_w \, d\phi - \int_{\phi_w}^{2\pi} \cos\phi \ln \overline{W}_w \, d\phi \quad (55)$$

If we define $\alpha_o = \alpha_{I_a + 1} = 0$, we can alter the indices to get

$$J_c - \pi = \sum_{i=1}^{I_a} \{\sin 2\alpha_i - \cos 2\alpha_{i+1})\} - \int_o^{\phi_w} \cos\phi \ln W_w \, d\phi - \int_{\phi_w}^{2\pi} \cos\phi \ln \overline{W}_w \, d\phi \quad (56)$$

Now equation (54) can be written as

$$K_H W_{cl} + \overline{K}_H W_{CI_a} + J_c - \pi = 0 \quad (57)$$

In a similar manner, if we define W_{si} as

$$W_{si} = \int_{\phi_{i-1}}^{\phi_i} \sin\phi \ln W_s (\phi) \, d\phi \quad (58)$$

and we define J_s as

$$J_s = \sum_{i=0}^{I_a} -(1+\cos 2\alpha_i) \ln (i,i) + (1+\cos 2\alpha_{i+1}) \ln (i,i+1) + \frac{1}{2} \phi_i (\cos 2\alpha_i - \cos 2\alpha_{i+1}) - \int_o^{\phi_w} \cos\phi \ln W_w \, d\phi - \int_{\phi_w}^{2\pi} \cos\phi \ln \overline{W}_w \, d\phi \quad (59)$$

Equation (30) can now be written as

$$K_H W_{SI} + \overline{K}_H W_{SI_a} + J_s = 0 \tag{60}$$

From equation (45),

$$\ln V_1 = \ln (i,i) - \ln (i,i+1) + \ln V_2 \tag{61}$$

Substituting this value of V_1 into equation (44) yields

$$\ln |\cos\alpha_{I_1}| - \ln (i,i) + \ln (i,i+1) + \ln V_2 - K_H \ln W_w(0)$$

$$= \ln |\cos\alpha_{I_a}| - \ln V_{I_a} - \overline{K}_H \ln \overline{W}_w (2\pi) \tag{62}$$

From equation (45), V_2 can be determined as a function of V_3, and so forth until V_{I_a} is reached. In this manner, V_1 and V_{I_a} are eliminated from (44) yielding

$$-K_H \ln W_w(0) + \overline{K}_H \ln \overline{W}_w (2\pi) + \sum_{i=0}^{\infty} \{-\ln (i,i) + \ln (i,i+1)\} = 0 \tag{63}$$

Defining J_T as being the summation term of this equation, equation (63) can be written as

$$-K_H \ln W_w(0) + \overline{K}_H \ln \overline{W}_w (2\pi) + J_T = 0 \tag{64}$$

We now have three equations (equations (57), (60), and (64)) for the three unknowns (K_H, $\overline{K}_H$ and ϕ_{i_L}). Eliminating K_H and $\overline{K}_H$ yields

$$(J_c - \pi) D_1 - J_s D_2 + J_T D_3 = 0 \tag{65}$$

where

$$D_1 = W_{s1} \ln \overline{W}_w (2\pi) + W_{SI_a} \ln W_w (0) \tag{66}$$

$$D_2 = W_{c1} \ln \overline{W}_w (2\pi) + W_{CI_a} \ln W_w (0) \tag{67}$$

$$D_3 = W_{c1} W_{sI_a} - W_{cI_a} W_{s1} \tag{68}$$

Equation (65) is a transcendental equation for ϕ_{I_L}. Once the value of ϕ_{I_L} is determined, K_H and $\overline{K}_H$ can be determined from equations (57) and (60).

With equation (45), we now have $I_a - 1$ equations for the I_a values of V_i. The last equation comes from the previously unused equation (29), which guarantees uniform flow at infinity.

$$\int_0^{2\pi} P(\phi)\, d\phi = \sum_{i=1}^{I_a} \left\{ \int_{\phi_{i-1}}^{\phi_i} \left[\ln\left|\cos\left(\frac{\phi}{2} - \alpha_i\right)\right| - \ln \frac{V_i}{V_1} \right.\right.$$

$$\left.\left. - K_H \ln W_s - \ln W_s(\phi) \right] d\phi \right\} + 2\pi(\ln 2 - \ln V_1) = 0 \tag{69}$$

Now that all of the ϕ_i's, K_H, and $\overline{K}_H$ are known, $P(\phi)$ can be calculated from equation (43), $Q(\phi)$ can be calculated from equation (34) and $x(\phi)$ $y(\phi)$ can be calculated from equations (32) and (33).

For practical numerical calculations, the circle plane is divided into 2N equal parts, with the positions given by

$$\phi = \tau_\nu = \frac{\nu\pi}{N} \qquad (\nu = 0, 1, 2, \ldots, 2N-1) \tag{70}$$

Next, the ϕ_i's (except ϕ_{i_L}) α_i's, K, $\overline{K}$, μ, and $\overline{\mu}$ are chosen. The values of W_{c1}, W_{CI_a}, W_{s1}, W_{SI_a} can then be calculated (equations (51) and (58)). Using equations (66) through (68), D_1, D_2, and D_3 can be calculated, and the transcendental equation can be established. Once ϕ_{I_L} is determined

K_H and $\overline{K}_H$ can be calculated from equations (57) and (60). $P(\phi)$ and $Q(\phi)$ can be determined at each point on the circle. Then $x(\phi)$ and $y(\phi)$ are determined, so 2N points are determined on the airfoil. These points are equally spaced on the circle plane, but they are not equally spaced in the airfoil plane.

The resulting coordinates will yield an airfoil oriented at its zero lift line. However, the angle between the zero lift line and the chord line (β) can be determined and subtracted from α to yield the angle of attack with respect to the chord line.

Since the values of K_H and $\overline{K}_H$ are determined by the closure requirements, there is no direct control of these values in the input specifications. K_H and $\overline{K}_H$ determine the trailing edge angle. In order to maintain some control over this trailing edge angle, a desired value of $K_s = K_H + \overline{K}_H$ can be specified, and by iteration, varying either α_i on the upper or lower surface (or both surfaces), or K or $\overline{K}$, the desired K_s can be attained.

III. THE STRATFORD DISTRIBUTION

The problem of high lift airfoils with a Stratford distribution was investigated by Ormsbee and Chen [2,3] in 1971. The lift of an airfoil is generally limited by boundary layer separation on the upper surface, where the fluid is subjected to an adverse pressure gradient. The usual velocity distribution on an airfoil generating lift is one in which the flow accelerates as it goes around the leading edge, reaches a maximum, and then decelerates as it approaches the trailing edge. The problem of separation occurs during this deceleration of the flow.

In order to achieve the maximum lift, we want to accelerate the flow on the upper surface to a maximum, hold this maximum velocity for as long as possible, and then decelerate the flow as quickly as possible without separation. This is similar to the problem investigated by Stratford in 1957 [6]. Stratford investigated flow over a flat plate, decelerating the flow by varying the shape of the wall facing the test surface. On an airfoil, the velocity gradient is developed by varying the shape of the airfoil, but the results should be the same no matter how the velocity gradient is obtained.

In developing the Stratford distribution, incompressible flow at a large Reynolds number is assumed. The lift, then, is given by the Kutta-Jowkowski theorem.

$$L = \rho U_\alpha \Gamma \tag{71}$$

Therefore, assuming a fixed density and free stream velocity, the only way to increase the lift is to increase the circulation. The circulation, Γ, is defined by

$$\Gamma = \int_0^{s_t} V(s)\,ds \tag{72}$$

where s is the distance from the trailing edge to the point in question measured clockwise along the surface of the airfoil, and s_t is the total length along the surface of the profile of the airfoil. V(s) is the local velocity on the surface of the airfoil. If we use the subscript L to indicate the stagnation point, the integral for Γ can be broken into two separate integrals

$$\Gamma = \int_0^{s_L} V(s)ds + \int_{s_L}^{s_T} V(s)ds \tag{73}$$

Along the lower surface, from s = 0 to $s = s_L$, the velocity is always in the direction of negative s. Therefore, $\int_0^{s_L} V(s)ds$ is negative, and the largest value possible is zero. This indicates the velocity along the lower surface is always zero, or stagnation occurs along the entire lower surface. Assuming zero velocity along the lower surface, the circulation can be given as

$$\Gamma = \int_{s_L}^{s_T} V(s)ds \tag{74}$$

For convenience, the origin of s may be shifted from the trailing edge to the front stagnation point, and the distance along the upper surface may be referred to as s_u, such that

$$s_u = s_T - s_L \tag{75}$$

In this case, equation (74) may be written as

$$\Gamma = \int_0^{s_u} V(s)ds \tag{76}$$

The lift can be normalized with respect to the free stream dynamic head and the length s_u of the upper surface.

$$C_L = \frac{L}{\frac{1}{2} \rho U_\infty^2 s_u} \tag{77}$$

and the velocity can be normalized with respect to the free stream velocity

$$q(s) = \frac{U(s)}{U_\infty} \tag{78}$$

Equation (71) can then be written as

$$C_L = \frac{2}{s_u} \int_0^{s_u} q(s) ds \tag{79}$$

As mentioned earlier, the velocity q(s) starts out as zero at the stagnation point, increases rapidly to a maximum velocity, then, starting at a point $s = s_0$, decreases as rapidly as possible without separation down to the trailing edge velocity. Boundary layer separation is imminent when the local skin friction goes to zero. Therefore, in order to have a maximum deceleration, we want to have a velocity gradient such that the skin friction is zero from $s = s_0$ to $s = s_u$.

Stratford derived an expression for flow over a flat plate with zero skin friction based on C_{p_0}, the pressure coefficient based on the pressure before the pressure rise begins.

$$C_{p_0} = \frac{p - p_t}{p_0 - p_t} = \frac{p}{\frac{1}{2} \rho U_0^2} \tag{80}$$

where p_t is the total pressure, p_0 is the static pressure before the pressure rise, p is the local pressure, and U_0 is the initial velocity. If we let the leading edge of the flat plate be the origin of coordinates,

so x = 0 at the leading edge, and let the pressure be constant until x_0, where it begins to rise, the local skin friction will be zero, according to Stratford, in the region of increasing pressure when

$$\left(2\,C_{p_0}\right)^{1/4(n-2)}\left(x\,\frac{d\,C_{p_0}}{dx}\right)^{1/2} = 1.06\,\beta(10^{-6}\,R_{e_x})^{1/10} \qquad (81)$$

β is a constant equal to about .66 for Reynolds numbers on the order of 10^6, R_{e_x} is the local Reynolds number based on U_0 and x, and n is about 6 or 7 for Reynolds numbers between 10^6 and 10^7. Equation (81) is not sensitive to the value of n, and a change in value of n = 6 to n = 7 will yield about 4 percent effect. Experimental data has indicated that a value of $n = \log_{10} R_{e_0}$, where R_{e_0} is the Reynolds number based on x_0 and U_0, yields an error of less than 1 percent.

Equation (81) was derived on the basis of an inner and an outer solution. However, at the point where $C_{p_0} = \frac{n-2}{n+1}$, the join of the inner and outer solutions reaches the outer edge of the boundary layer when idealized velocity profiles are used, and the equation is no longer valid.

Equation (81) is a differential equation for $C_{p_0}(x)$ resulting in the desired zero skin friction velocity gradient. The solution of this equation yields

$$C_{p_0}\left(\frac{x}{x_0}\right) = 0.645\,\{0.435\,R_{e_0}^{1/5} - 1]\}^{2/n} \quad C_{p_0} \geq \frac{n-2}{n+1} \qquad (82)$$

Stratford extended the range of C_{p_0} beyond $C_{p_0} = \frac{n-2}{n+1}$ by assuming a constant shape factor, $H = \frac{\delta^*}{\theta}$. Using this assumption, C_{p_0} is defined by

$$C_{p_0} = 1 - \frac{a}{(x+b)^{1/2}} \qquad C_{p_0} < \frac{n-2}{n+1} \qquad (83)$$

where a and b are constants such that C_{p_0} and $\frac{d C_{p_0}}{dx}$ are continuous at $C_{p_0} = \frac{n + 2}{n - 1}$. Stratford [10] conducted a series of experiments that showed that equations (82) and (83) do indeed yield a near zero value for the skin friction at the surface.

Rather than work with the pressure coefficient, we will work with the normalized velocity, q(s). To make the conversion, we use the relationship

$$C_{p_0} = 1 - \left(\frac{U}{U_0}\right)^2 \tag{84}$$

and the relationship

$$q = \frac{U}{U_\infty} = \frac{U}{U_0} = \frac{U_0}{U_\infty} = q_0 \frac{U}{U_0} \tag{85}$$

Therefore,

$$q = q_0 \left[1 - C_{p_0}\left(\frac{x}{x_0}\right)\right]^{1/2} \tag{86}$$

Equation (79) can now be written as

$$C_L = \frac{2}{s_u} \int_0^{s_u} q(s)ds + \int_{s_0}^{s_u} q_0 \left[1 - C_{p_0} \frac{x}{x_0}\right]^{1/2} ds \tag{87}$$

We now need the relationship between x and s. Along the flat plate, x is the coordinate, while s is the coordinate along the surface of the airfoil. In order to relate the two, we set the momentum thickness of the boundary layer at $s = s_0$ equal to the momentum thickness of the boundary layer at $x = x_0$ is then

$$x_0 = \int_0^{s_0} \left(\frac{U(s)}{U_0}\right)^3 ds \tag{88}$$

The relation between s and x must be such that s_0 and x_0 occur at the same location. If we define the constant k such that

$$k = \frac{s_0}{x_0} \tag{89}$$

the relation between x and s becomes

$$s = x + (k-1)\, x_0 \tag{90}$$

or

$$x = s - (k-1)\, x_0 \tag{91}$$

We can now define a new variable z such that

$$z = \frac{x}{x_0} = \frac{s}{x_0} - (k-1) \tag{92}$$

With this relation, equation (88) can be written

$$1 = \int_{1-k}^{1} \left(\frac{q(z)}{q_0}\right)^3 dz \tag{93}$$

We will use the notation Z to indicate the value of z at $s = s_u$.

With this notation, equation (87) can be written as

$$C_L = \frac{2}{Z+k-1} \left\{ \int_{k-1}^{1} q(z)dz + q_0 \int_{1}^{Z} [1 - C_{p_0}(z)]^{1/2} dz \right\} \tag{94}$$

The problem is to achieve a maximum C_L from equation (94). The length of the upper surface (s_u) is a factor that will be fixed by the desired chord length of the airfoil and C_{p_0} is a function of R_{e_0}, which is a function of the free stream Reynolds number, and is, therefore, a design parameter to be specified for the airfoil.

Therefore, in order to maximize the lift, there are three variables in equation (94) that can be altered to maximize the lift. In the first integral, $q(z)$ has no limitation other than it is non-decreasing. In the second term, q_0, the maximum velocity on the upper surface, has not been specified. The third variable which is implicit in equation (94) is s_0, the location of the beginning of the pressure rise.

The first integral will be maximized if $q(z)$ is a maximum. This indicates that $q(z)$ should accelerate instantaneously to the valve q_0 and remain there until $s = s_0$. This means that equation (93) is now

$$1 = \int_{1-k}^{1} dz \tag{95}$$

so $k = 1$. The instantaneous acceleration of the velocity after the stagnation point indicates that the stagnation point is on the leading edge, which results in a sharp leading edge, which will yield poor results in off-design angles of attack. More will be said about this in a later chapter.

As can be seen from equation (83), C_{p_0} reaches the value unity only at infinity. Since the chord length of infinity is not feasible, a non-zero trailing edge velocity will be accepted, which will be referred to as q_u. This leads to a sharp trailing edge, which is acceptable for our purposes. Therefore, there are now three values that can be varied to lead to a maximum C_L, q_0, q_u, and s_0. These three quantities are not independent: once two of them have been determined, the third is also determined once R_{e_0} and s_u are specified. Therefore, if the value of one of these quantities is specified, one of the other quantities may be varied to obtain a maximum C_L, and the third value will be uniquely defined.

If s_0 is specified, for any value of q_0 a q_u will result. However, as q_0 increases, C_L increases, and there is no upper limit. If q_0 is fixed, the C_L increases as S_0 increases, and reaches a maximum when $s_0 = s_u$, or there is no recovery at all, and $q_0 = q_u$. This is not a satisfactory solution. The only remaining possibility is to fix q_u and vary q_0 and s_u to get a maximum C_L.

The function C_{p_0} can take either the form of equation (80) or the form of equation (83), depending on the values of R_{e_0} and $\frac{x}{x_0}$. For the values of R_{e_o} normally encountered in airfoils, C_{p_0} will reach the value $\frac{n-2}{n+1}$ soon after the pressure recovery begins. The point at which this occurs will be referred to as s_m (or z_m or x_m, depending on the coordinate system used).

If the notation

$$a' = \frac{a}{\sqrt{X_0}} \tag{96}$$

$$b' = \frac{b}{\sqrt{X_0}} \tag{97}$$

is used, equation (83) can be written

$$C_{p_0}(z) = 1 - \frac{a'}{(z+b')^{1/2}} \qquad C_{p_0} < \frac{n-2}{n+1} \tag{98}$$

At the trailing edge, $z = Z$

$$C_{p_0}(Z) = 1 - \frac{a'}{(Z+b')^{1/2}} \tag{99}$$

or, using equation (86)

$$q_u = q_0 \sqrt{\frac{a'}{(Z+b')^{1/2}}} \tag{100}$$

This can be rearranged to

$$q_0 = \frac{q_u}{\sqrt{a'}} (Z + b')^{1/4} \tag{101}$$

Therefore, equation (94) can be rewritten as

$$C_L = \frac{2\, q_u (Z+b')^{1/4}}{Z+k-1\ \sqrt{a'}} \left\{ 1 + \int_1^{z_m} \left[1 - 0.645(0.435\, R_{e_0}^{1/5} (z^{1/5} - 1))^{2/N} \right]^{1/2} dz + \int_{z_m}^{Z} \frac{dz}{(z+b')^{1/4}} \right\} \tag{102}$$

Since z_m depends only on R_{e_0}, the first integral is a function only of R_{e_0} and can be abbreviated as

$$I(R_{e_0}) = \int_1^{z_m} \left[1 - 0.645(0.435\, R_{e_0}^{1/5} (z^{1/5} - 1))^{2/N} \right]^{1/2} dz \tag{103}$$

By carrying out the integration in the last term in equation (100) and utilizing the fact that $k = 1$,

$$C_L = \frac{2\, q_u (z+b')^{1/4}}{Z\ \sqrt{a'}} \left\{ 1 + I(R_{e_0}) + \frac{4}{3} \sqrt{a'} \left[(Z+b')^{3/4} - (z_m - b')^{3/4} \right] \right\} \tag{104}$$

If R_{e_0} and q_u are specified, C_L varies only with z. Therefore, the maximum value of C_L occurs at a value of z where the first derivative of C_L with respect to z is zero. Taking the derivative and setting it equal to zero yields

$$3/4 \left[1 + I(R_{e_0}) - \frac{4}{3} \sqrt{a'} (Z_m+b)^{3/4} \right] (Z+b') + \frac{4}{3} \sqrt{a'}\, b' (Z+b')^{3/4} + \frac{b'}{4} \left[1 + I(R_{e_0}) - \frac{4}{3} \sqrt{a'} (z_m+b')^{3/4} \right] = 0 \tag{105}$$

Equation (105) is a fourth degree algebraic equation for $(Z+b')^{1/4}$, and, as such, yields four roots for $(Z+b')^{1/4}$. For Reynolds numbers in the range of airfoils for General Aviation aircraft, there are two complex roots, one positive root, and one negative root. The only root that is physically meaningful is the positive real root. By looking at the value of the second derivative, it can be shown that the positive root does indeed yield a maximum C_L. Substituting the value of $(Z+b')^{1/4}$ back into equation (101) yields q_0 as a function of q_u, and, by solving

$$Z = \frac{s_u}{x_0} \tag{106}$$

for x_0, s_0 can be determined. Therefore, the variational problem has been solved.

Up to this time, it has been assumed that the flow in the boundary layer has been fully turbulent from the stagnation point to the point of initial pressure recovery. However, in actual flows, the flow will be initially laminar, and will transition to a turbulent flow at some point beyind the stagnation point. With laminar flow present in the initial boundary layer, equation (88) is no longer valid, but will be replaced by

$$x_0 = 38.2 \left(\frac{\nu}{s_t U_t}\right)^{3/8} \left(\frac{U_0}{U_t}\right)^{1/8} \left[\int_0^{s_t} \left(\frac{U}{U_0}\right)^5 d\left(\frac{s}{s_t}\right)^{5/8} s_t\right] + \int_{s_t}^{s_0} \left(\frac{U}{U_0}\right)^3 ds \tag{107}$$

where the subscript t indicates the variable is evaluated at the transition point. Equation (107) assumes an instantaneous transition with a continuous momentum thickness at s_t. The point s_t can occur at s_0, but

the purposes of this paper, we will assume that s_t is not greater than s_0, as Stratford only considered the separation of fully turbulent flows.

If g is defined as

$$g = \frac{s_t}{s_0} \tag{108}$$

and s is replaced by z, as in the case of fully turbulent flows, equation (106) can be written

$$1 = 38.2 \left(\frac{\nu}{x_0 U_0}\right)^{3/8} (gk)^{5/8} + (1-g)k \tag{109}$$

In the case of the initially laminar boundary layer, another value is required, namely $R_{e_{cr}}$, the Reynolds number at transition. $R_{e_{cr}}$ will be defined as

$$R_{e_{cr}} = \frac{s_t U_0}{\nu} = \frac{g\, s_0\, U_0}{\nu} = \frac{g\, k\, x_0\, U_0}{\nu} \tag{110}$$

Note that the maximum velocity on the airfoil is used to define $R_{e_{cr}}$, rather than the free stream velocity. Rearranging terms, we get

$$g\, k = \frac{R_{e_{cr}}\, \nu}{x_0\, U_0} = \frac{R_{e_{cr}}}{R_{e_o}} \tag{111}$$

Substituting equation (110) into equation (108) yields

$$k = 1 - 38.2\, R_{e_0}^{-1}\, R_{e_{cr}}^{5/8} + \frac{R_{e_{cr}}}{R_{e_0}} \tag{112}$$

For the case of flow that is fully laminar until the pressure recovery starts, $s_t = s_0$ and $g = 1$. Therefore equation (111) becomes

$$k = \frac{R_{e_{cr}}}{R_{e_0}} \tag{113}$$

Substituting this into (111) yields

$$0 = 1 - 38.2\, R_{e_0}^{-1}\, R_{e_{cr}}^{5/8} \tag{114}$$

or

$$R_{e_0} = 38.2\, R_{e_{cr}}^{5/8} \tag{115}$$

Hence,

$$R_{e_{cr}} = \frac{1}{38.2}\, R_{e_0}^{8/5} \tag{116}$$

This indicates that for R_{e_0} greater than 1.655×10^4, $R_{e_{cr}}$ can be larger than R_{e_0}, even though s_0 is greater than s_t.

Once again, to find the maximum C_L, the derivative of C_L with respect to z needs to be set to zero. However, in this case, k is not equal to one, but is determined by equation (112). Taking the derivative of (102), using equation (103) to define $I(R_{e_0})$, and setting the result equal to zero yields

$$\frac{3}{4}\left|K + I(R_{e_0}) - \frac{4}{3}\sqrt{a'}\,(z_m+b')^{3/4}\right|(Z+b') - \frac{4}{3}\sqrt{a'}\,(K-1-b')(Z+b')^{3/4}$$

$$-\frac{1}{4}(K-1-b')\left|K + I(R_{e_0}) - \frac{4}{3}\sqrt{a'}\,(Z+b')^{3/4}\right| = 0 \tag{117}$$

As in the case of fully turbulent flow, this is a fourth degree algebraic equation for $(Z+b')^{1/4}$. The roots for R_{e_o}'s of interest here are similar to those of the fully turbulent case, and the single real positive root yields the maximum C_L. The difference between the fully turbulent velocity distribution and the partially laminar velocity distribution is the location of the start of the pressure recovery. For the partially laminar flow, s_0

is greater than the s_0 of the fully turbulent flow. Therefore, for equal R_{e_0}, s_u, and q_u, an airfoil with partially laminar flow will yield a slightly higher $C_{L_{max}}$.

IV. USING THE EPPLER METHOD TO DEVELOP A STRATFORD AIRFOIL

In the design of an airfoil, the first parameter to be chosen is an approximate value for q_u, the velocity at the trailing edge. The higher the q_u, the higher the C_L of the airfoil, but, also, the greater the angle of the trailing edge. The chord Reynolds number is dependent on R_{e_0} and q_u, so the choice of R_{e_0} will be dependent on the desired chord Reynolds number and q_u. By study of Tables 1 through 3 and with foresight gained through experience, an approximate R_{e_0} can be determined. This value can be modified during the design process until the desired chord Reynolds number is obtained.

If the airfoil is to have partially laminar flow along the rooftop, $R_{e_{cr}}$ will have to be chosen. One possible choice for $R_{e_{cr}}$ would be the critical Reynolds number for a flat plate, which, according to Schlicting [10] is 3.2×10^5. From equation (112), K can now be determined. By setting $C_{p_0} = \frac{n-2}{n+1}$ and solving equation (82) for $\frac{x}{x_0}$, z_m can be determined. a and b are now determined such that C_{p_0} and $\frac{dC_{p_0}}{dx}$ are continuous at $C_{p_0} = \frac{n-2}{n+1}$. Equation (117) can then be solved for $(Z+b')^{1/4}$, which determines Z. By substituting this value of Z into equation (101), the ratio between q_u and q_0 is determined. However, the exact value of q_0 or q_s is not known until the Eppler problem is solved. Using equations (90) and (106), the relation between x_0 and X can be determined as

$$X_0 = \frac{1}{Z + (K-1)} \tag{118}$$

where x_0 is non-dimensionalized with s_u.

Since the relation between x and ϕ is not known until after the solution of the Eppler problem, the location of the start of the pressure

recovery is not known in terms of the coordinates used to specify the input to the Eppler problem. However, using the approximation

$$x \approx \frac{1}{2}(1 + \cos\phi) \tag{119}$$

an approximate value of ϕ_w can be obtained as

$$\cos\phi_w \approx 2\, s_0 - 1 \tag{120}$$

where $s_0 = K\, x_0$.

In figure 3, if the initial slope of W_w (w') and the value of W_w at $\phi = 0$ are specified, the values of K and μ in equation (39) will be fixed. The value of ϕ_s, the start of the cusped region at the trailing edge, should be chosen as small as possible while maintaining a reasonable trailing edge angle and airfoil thickness. An approximate range of values of ϕ_s is 2° to 30°. The upper limit corresponds to higher values of q_u.

The values of $\overline{\phi}_w$, $\overline{w}'$, $\overline{w}$, and $\overline{\phi}_s$ on the lower surface must also be specified. Since the primary interest is in the pressure distribution on the upper surface at the design angle of attack, these values are not critical, but they can be altered to obtain better performance at off-design conditions. More will be said about this in the next chapter. In equation (39), K_H cannot be specified, as it will be determined by the solution to the problem. However, the solution can be iterated by varying either α^* or K (or $\overline{K}$) on the upper or lower surface (or both surfaces) until $K_H + \overline{K}_H = K_s$, a previously determined value. This allows control over the trailing edge angle. For the purposes of this paper, α^* will be allowed to vary on the lower surface.

The next design criteria to be chosen are the angles of attack. All of the angles of attack in the Eppler problem are referred to the zero lift line, rather than the chord line. The angle of attack on the upper surface will be the design angle of attack. This is the parameter that will control the velocity on the upper surface. The value required to obtain the desired approximate q_u can be determined by study of Tables 1 and 3. The angles of attack on the upper and lower surface must meet the requirements of equation (47).

It has been found through experience that it is impossible to match the initial slope of the pressure recovery of the Eppler output to the Stratford output with a continous angle of attack along the upper surface. However, by specifying a lower angle of attack in the region of the initial pressure recovery, the pressure distributions can be matched. This means the airfoil must be broken into four regions. In the first region, $0 = \phi_0 \leq \phi < \phi_1$, α^* will be the design angle of attack. In the second region, $\phi_1 \leq \phi < \phi_2 = \phi_w$, α^* will be less than the design angle of attack. In the region $\phi_2 \leq \phi < \phi_3 = \phi_{I_L}$, the α^* will again be equal to the design angle of attack. In the last region, which is the lower surface, $\phi_3 \leq \phi \leq \phi_4 = 2\pi$, α^* will be the angle of attack on the lower surface.

Using the input data derived above, the Eppler problem is solved, and maximum velocity on the upper surface and s_u, the surface length on the upper surface are determined. Using these values and the R_{e_0}, q_u/q_o, z_m, x_0, a', and b' determined earlier, a Stratford distribution is generated. By comparison the Stratford pressure distribution with the Eppler pressure distribution, the necessary changes to the Eppler input can be determined.

The primary variables to be changed are ϕ_w, which changes the location of the pressure recovery, w, which changes the trailing edge velocity, w' and α_2, which changes the initial slope of the pressure recovery, and ϕ_1, which changes the pressure distribution after the initial pressure drop.

These changes are input into the Eppler problem, and a new airfoil is generated. Since this airfoil will have a different maximum velocity on the upper surface and the stagnation point will be at a different location, changing the value of s_u, a new Stratford distribution will be needed, and the cycle repeats itself until an airfoil is generated that matches the corresponding Stratford distribution. Determining how much to change each input variable to get a desired change in the output of the Eppler problem is an art that can be learned only by experience.

Table 1 shows the variation of several airfoils with varying design angle of attack and varying K_s. Table 2 shows the variation with varying R_{e_0}. These airfoils are labelled by a number which gives some of the pertinent information about that airfoil. The first two digits indicate the free stream Reynolds number ($\times 10^{-5}$) of the airfoil. The second pair of digits represent the C_L ($\times 10$) of the airfoil as indicated by the Eppler program. The third pair of digits is $R_{e_{cr}}/R_{e_{chord}}$ ($\times 10^2$). This is the location (in terms of s) of the transition point. The fourth pair of digits is $\frac{1}{q_o}$ ($\times 10^2$), which is the free stream Mach number where flow on the rooftop first becomes sonic. The last pair of digits is the thickness of the airfoil in percent of the chord length. Thus, an airfoil labelled 1640-20-34-21 indicates an airfoil with a design

TABLE 1

VARIATION OF DESIGN INPUTS WITH VARYING ANGLE OF ATTACK AND K_s

Airfoil	Design angle of attack	ϕ_w	w	α_2	ϕ_1	K_s
1640-20-34-14	34.00	36.73	5.04	10.00	35.10	45.00
1642-20-33-15	36.00	37.60	5.07	11.90	35.60	55.00
1543-21-33-18	36.00	38.00	5.13	3.00	36.85	115.00
1447-23-31-15	40.00	39.00	5.14	7.00	37.50	65.00
1447-23-32-16	40.00	39.00	5.18	2.00	37.90	85.00
1348-25-31-17	40.00	39.60	5.19	2.00	38.65	115.00
1449-23-31-16	42.00	40.00	5.15	8.00	38.50	70.00
1350-23-31-17	42.00	40.00	5.18	5.00	38.75	90.00
1350-23-30-18	42.00	40.40	5.22	2.00	39.40	115.00
1350-23-28-19	42.00	40.50	5.26	-0.90	39.80	135.00
1351-23-30-16	44.00	41.00	5.16	9.00	39.50	75.00
1352-25-30-17	44.00	41.00	5.26	6.00	39.70	95.00
1352-25-29-17	44.00	41.00	5.35	3.00	39.90	115.00
1253-26-29-19	44.00	41.75	5.28	7.00	40.50	135.00
1254-27-29-18	46.00	42.00	5.40	6.00	40.70	115.00
1254-29-27-19	46.00	42.45	5.40	9.00	40.90	135.00
1156-29-27-18	48.00	43.00	5.46	7.00	41.70	125.00
1256-29-27-17	48.00	43.00	5.46	6.00	41.80	135.00
1256-27-28-18	48.00	43.50	5.50	9.75	41.95	145.00
1157-29-27-19	48.00	43.70	5.49	9.75	42.20	155.00
1157-29-28-19	48.00	43.80	5.53	9.00	42.35	165.00
1157-29-27-20	48.00	43.90	5.56	8.50	42.50	175.00

TABLE 2

VARIATION OF DESIGN INPUTS WITH VARYING R_{e_0}

Airfoil	R_{e_0}	ϕ_w	w	α_2	ϕ_1	K_s
1256-27-28-18	1.56	43.50	5.50	9.75	41.95	145.00
1357-25-28-19	1.90	43.10	5.45	9.75	41.40	145.00
1657-20-28-19	2.40	42.90	5.42	9.75	41.20	145.00
1857-18-28-19	2.65	42.80	5.39	9.75	41.05	145.00
2057-16-28-19	3.00	42.50	5.41	9.75	40.75	145.00
2257-15-28-19	3.40	42.10	5.36	8.75	40.40	145.00
2557-12-28-20	4.00	42.10	5.37	9.75	40.35	145.00
2857-12-27-20	4.50	42.00	5.32	9.75	40.30	145.00
3157-10-28-20	5.00	41.70	5.30	6.00	40.40	145.00
3757-08-28-20	6.00	41.05	5.31	6.00	39.50	145.00
4057-08-28-21	6.70	41.10	5.27	9.75	39.10	145.00
4557-07-29-20	7.50	41.05	5.29	9.75	39.25	145.00
5157-06-28-22	9.00	40.85	5.22	9.75	38.80	145.00
2256-15-29-19	3.40	42.05	5.33	8.75	40.35	130.00
2057-16-28-19	3.00	42.25	5.41	7.75	40.65	135.00

TABLE 3

VARIATION OF SELECTED PARAMETERS

Airfoil	q_u	q_0	α_4	ϕ_{I_L}	k_s	C_L
1640-20-34-14	1.385	2.907	15.31	56.49	3.423	3.591
1642-20-33-15	1.418	2.990	22.30	59.14	4.076	
1543-21-33-18	1.462	3.104	17.72	57.73	6.888	
1447-23-31-15	1.493	3.173	26.57	61.02	4.835	
1447-23-32-16	1.506	3.219	25.08	60.51	5.758	
1348-25-31-17	1.538	3.249	23.43	60.00	7.185	
1350-23-31-17	1.548	3.301	27.53	61.57	6.159	4.012
1350-23-30-18	1.569	3.357	25.83	60.99	7.323	
1350-23-28-19	1.588	3.371	24.66	60.62	8.269	
1351-23-30-16	1.571	3.374	30.96	62.97	5.621	4.338
1352-25-30-17	1.589	3.401	29.83	62.57	6.560	
1352-25-29-17	1.611	3.413	28.87	62.24	7.505	
1253-26-29-19	1.626	3.470	27.42	61.75	8.431	
1254-27-29-18	1.650	3.489	31.73	63.45	7.694	4.053
1254-29-27-19	1.666	3.513	30.60	63.06	8.626	
1156-29-27-18	1.691	3.580	33.89	64.42	8.341	
1256-29-27-17	1.690	3.620	32.94	64.06	8.782	
1256-27-28-18	1.710	3.598	32.95	64.09	9.278	
1157-29-27-19	1.719	3.615	32.37	63.89	9.741	
1157-29-28-19	1.729	3.636	31.74	63.66	10.200	
1157-29-27-20	1.737	3.651	31.11	63.44	10.670	3.985
1357-25-28-19	1.696	3.615	32.44	63.90	9.242	
1657-20-28-19	1.692	3.605	32.38	63.88	9.238	
1857-18-28-19	1.684	3.624	32.04	63.75	9.217	
2057-16-28-19	1.684	3.599	32.19	63.81	9.224	
2257-15-23-19	1.673	3.588	31.96	63.73	9.203	
2557-12-28-20	1.675	3.571	32.15	63.81	9.209	
2857-12-27-20	1.668	3.570	32.01	63.76	9.194	
3157-10-28-20	1.660	3.571	31.80	63.69	9.182	
3757-08-28-20	1.648	3.562	31.46	63.57	9.156	
4057-08-28-21	1.641	3.569	31.25	63.49	9.143	
4557-07-29-20	1.643	3.563	31.33	63.52	9.148	4.140
5157-06-28-22	1.630	3.571	30.93	63.37	9.122	

free stream Reynolds number (based on the chord length) of 1.6 million, a design C_L of 4.0, boundary layer transition at s/chord length = .20, a critical Mach number of .34, and a thickness of 21 percent.

The airfoil is divided into small segments that are of equal length in the circle plane. For the purposes of this study, the circle was divided into 92 segments, but more or fewer points could have been used. As the number of points is increased, the accuracy of the problem increases, but the number of calculations also increases. The data relating to a position on the airfoil (all the ϕ data) is given in terms of these circle divisions. The relation between a value of ϕ given in degrees and the same value of ϕ given in circle divisions is

$$\phi \text{ (circle divisions)} = \phi \text{ (degrees)} \times \frac{\text{number of circle divisions}}{360} \tag{121}$$

The data in Tables 1 to 3 is given in this form.

In column 2 of Table 1, the design angle of attack is listed. The dependence of the trailing edge velocity, listed in Table 3 column 1 can be noted here. In column 2 of Table 2, the R_{e_0} of different airfoils is listed. The design angle of attack of the airfoils in Table 2 is 48°, and the R_{e_0} of the airfoils in Table 1 is 1.56 million. Column 3 in both tables lists ϕ_w, the start of the pressure recovery and column 4 lists w, the value of W_w at $\phi = 0$. If the entire upper surface were at the design angle of attack, this would be the same as q_u/q_0. However, the discrepancy is caused by the short segment after the initial pressure recovery, where α^* is much lower. This second angle of attack is listed in column 5, and ϕ_1 is listed in column 6. The value of α^* is α_2 in the range $\phi_1 \leq \phi < \phi_w$. Column 7 lists K_s, which is the value $K_H + \bar{K}_H$ iterates to.

For the remainder of the design inputs, the following values were used:

$\phi_s = 1.5$

$w' = 50.00$

$\overline{\phi}_w = 30.00$

$\overline{\phi}_s = 4.99$

$\overline{w}' = 80.00$

$R_{e_{cr}} = 3.2 \times 10^5$

Table 3 lists some of the results of the above input data. Column 4 lists α^* on the lower surface. Although this value is determined through iteration in the program, if the initial guess is as close as possible to the final result, fewer iterations are required. Column 5 lists ϕ_{I_L}, which is referred to as the stagnation point. In actuality, this has no physical meaning, as it is the stagnation point when each section of the airfoil is at its own α_i. The stagnation point of the airfoil at any one angle of attack will be different than ϕ_{I_L}.

Column 6 lists the C_L as obtained from the Lockheed [11] program. This check was not run for all the airfoils, so this list is not complete. Of those that were run, the values of C_L did not agree with the C_L predicted by the Eppler program. This is apparently due to the inability of the flow to make the sudden recovery at the trailing edge. In the next chapter, an improvement will be suggested that should yield better results.

A typical airfoil is shown in figure 4. Figure 5 portrays the pressure distribution of this airfoil, and figure 6 is the equivalent

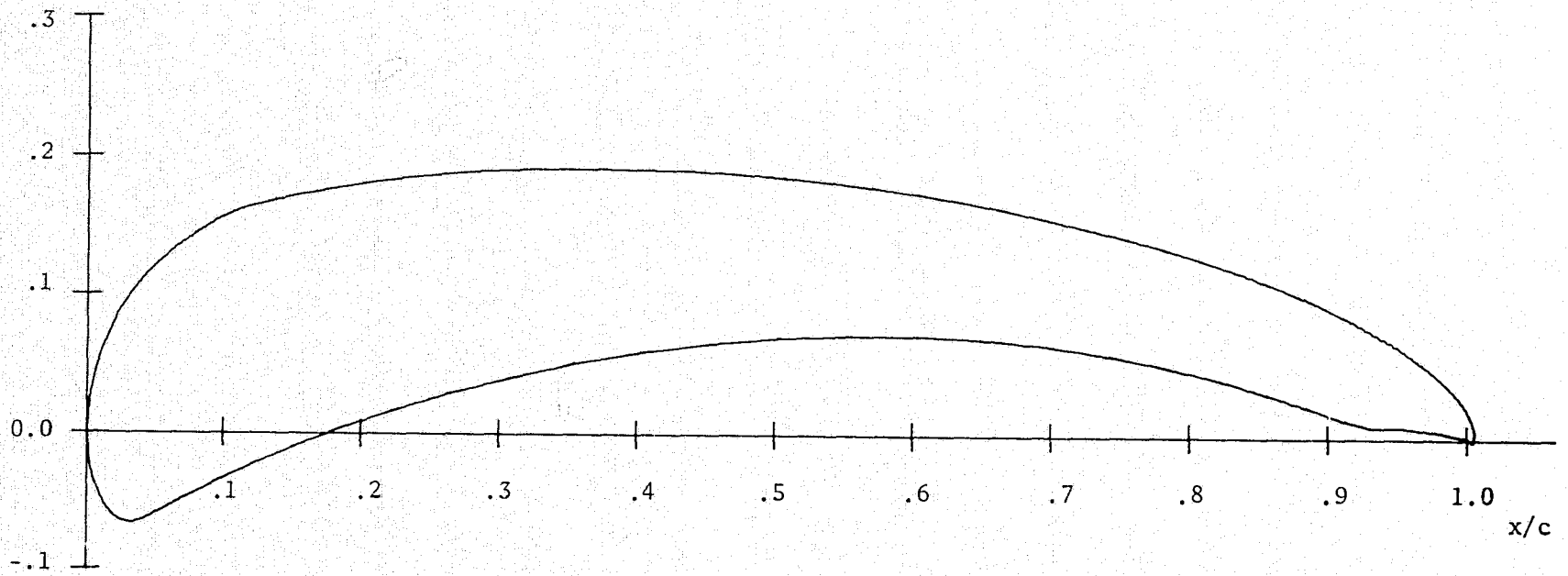

Figure 4. U of I HLE 1657-20-28-19 Airfoil

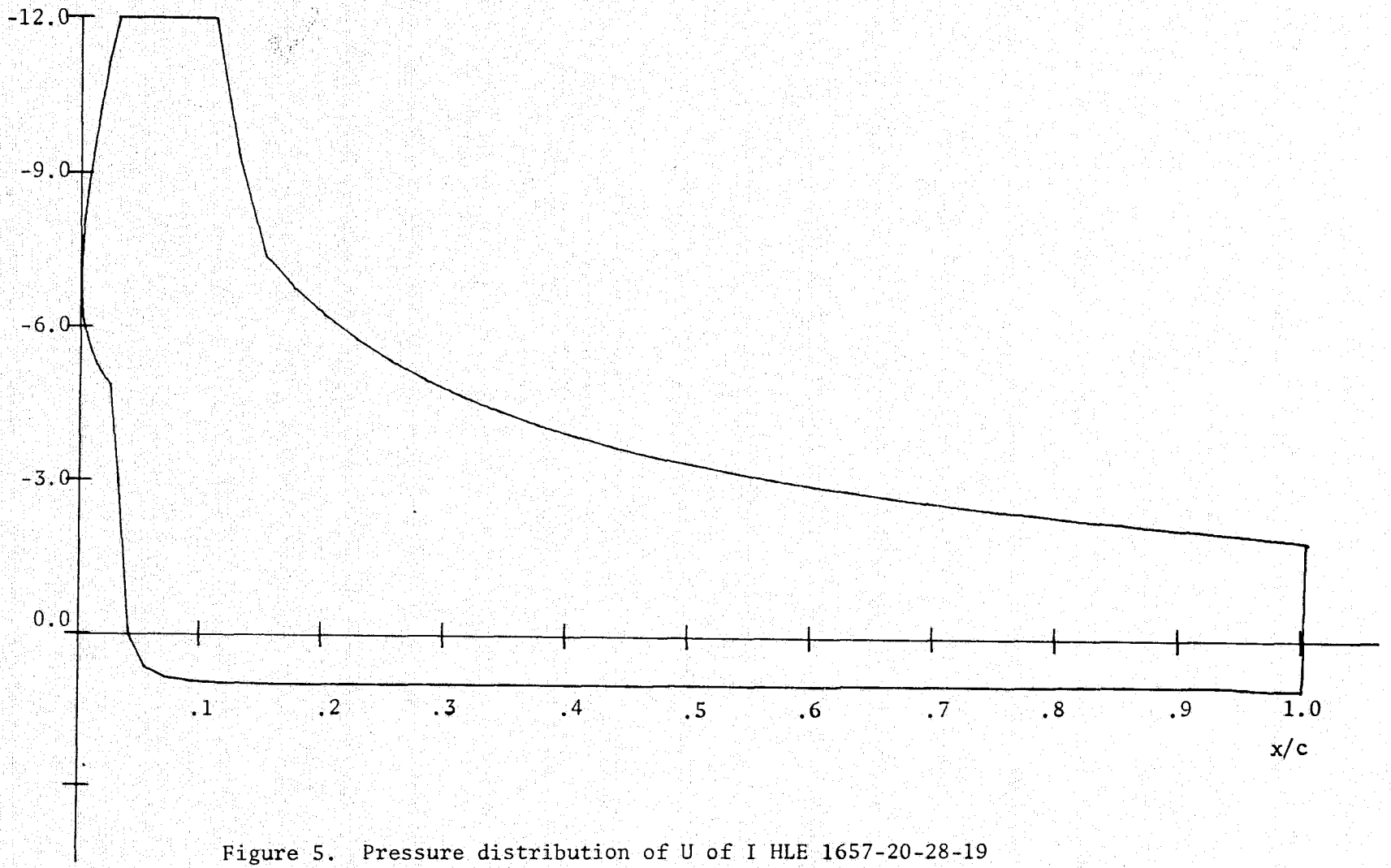

Figure 5. Pressure distribution of U of I HLE 1657-20-28-19

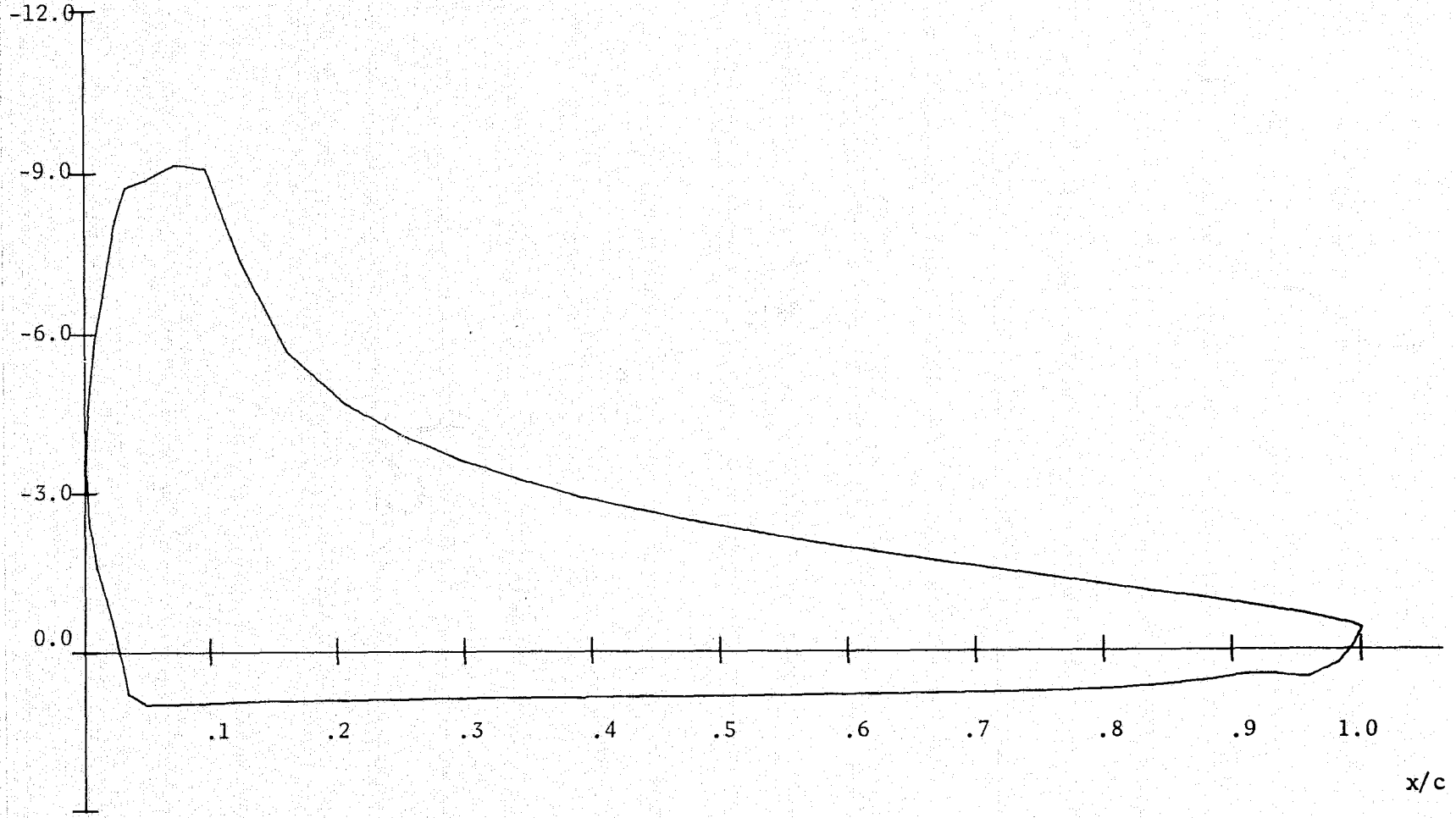

Figure 6. U of I HLE 1657-20-28-19 Lockheed pressure distribution

pressure distribution from the Lockheed program. It can be noted that the rooftop pressure distribution is not nearly as negative with the Lockheed distribution as it is with the Eppler distribution. This is typical of all the airfoils tested with the Lockheed program. Figures 7 and 8 show several more airfoil profiles and pressure distributions.

In figure 4, a small protuberance can be noted at the trailing edge on the lower surface. This is typical of the airfoils with the higher trailing edge velocity, and is apparently due to the trailing edge angle becoming extremely large (greater than 180°) In many cases, this protuberance caused a failure of the Lockheed program due to the method of determining the chord line in this program. The Lockheed program starts at the trailing edge and moves along the lower surface until it finds a point where the distance from the trailing edge to to the point is less than the distance from the trailing edge to the previous point. This can occur in the region of the protuberance, which leaves too few points on the lower surface for a reasonable solution. This problem can be eliminated by smoothing the protuberance out of the profile. By comparing results before and after smoothing with airfoils that did work in the Lockheed program, it was found that this protuberance had very little effect on the results of the Lockheed program. A method of eliminating this protuberance will be suggested in the next chapter.

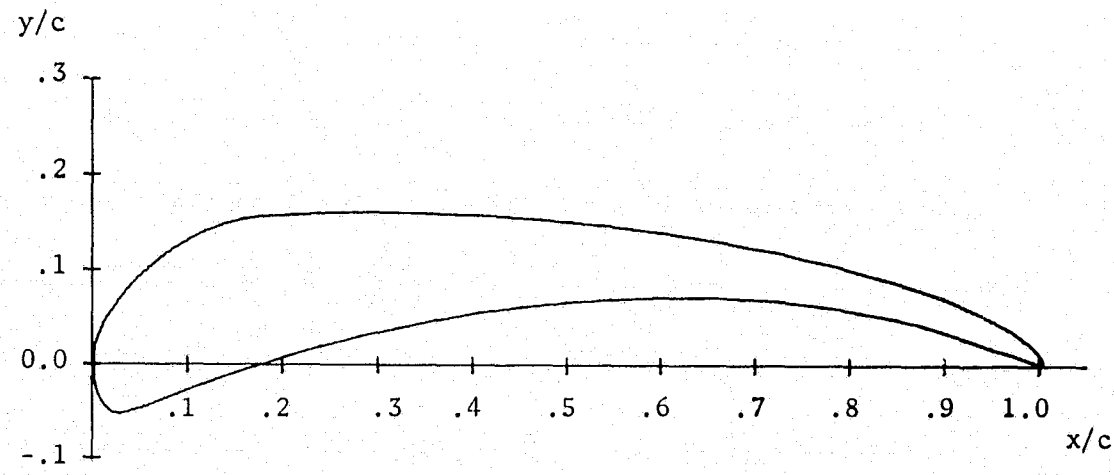

U of I HLE 1447-23-32-16

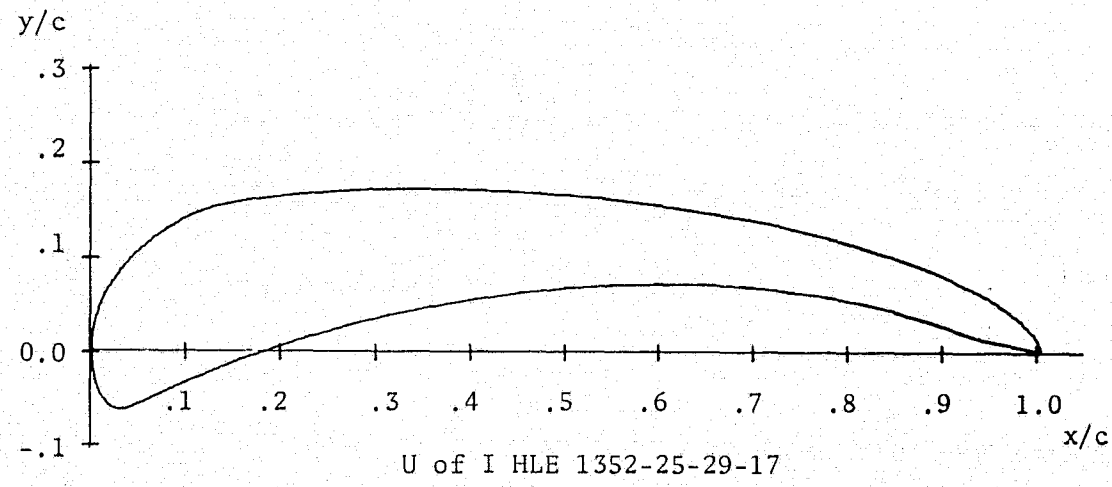

U of I HLE 1352-25-29-17

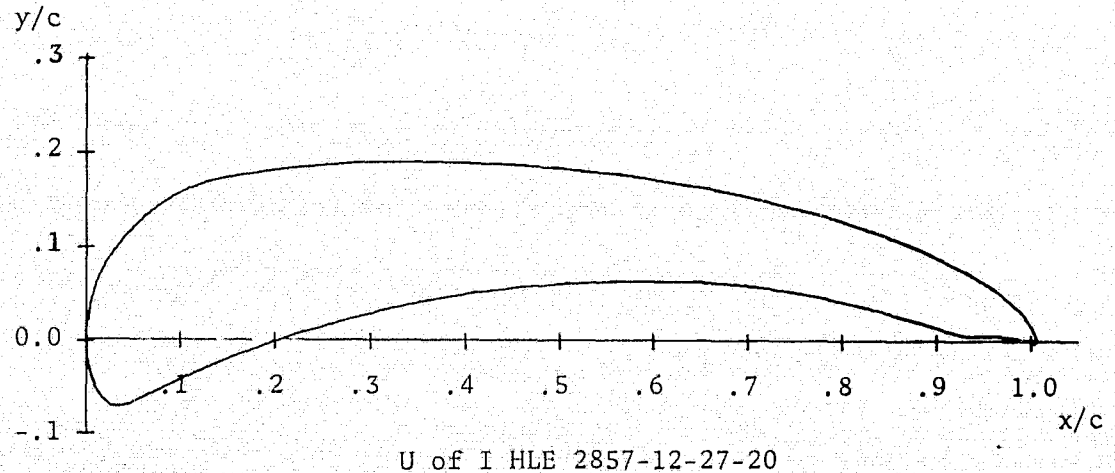

U of I HLE 2857-12-27-20

Figure 7. Several airfoils

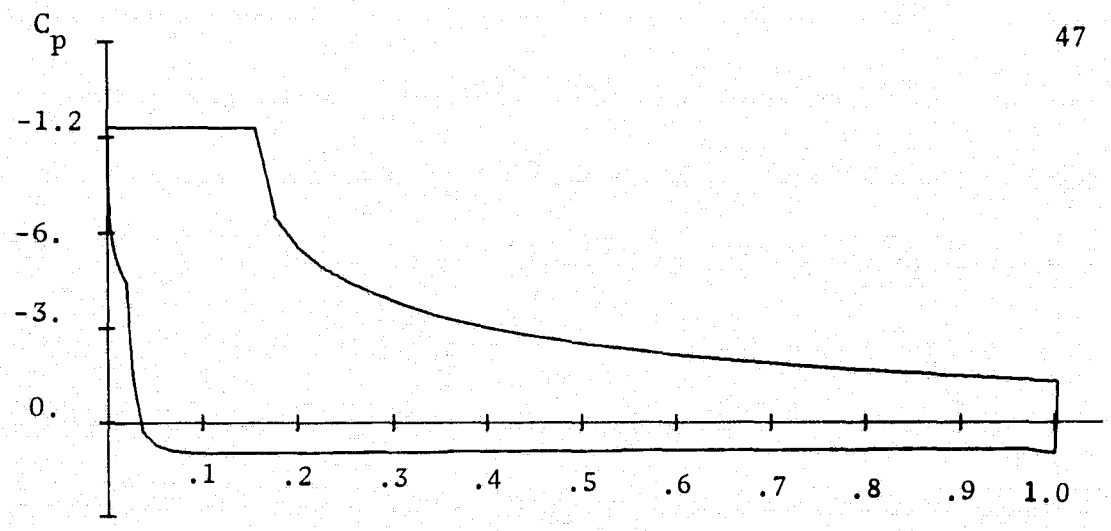

U of I HLE 1447-23-32-16

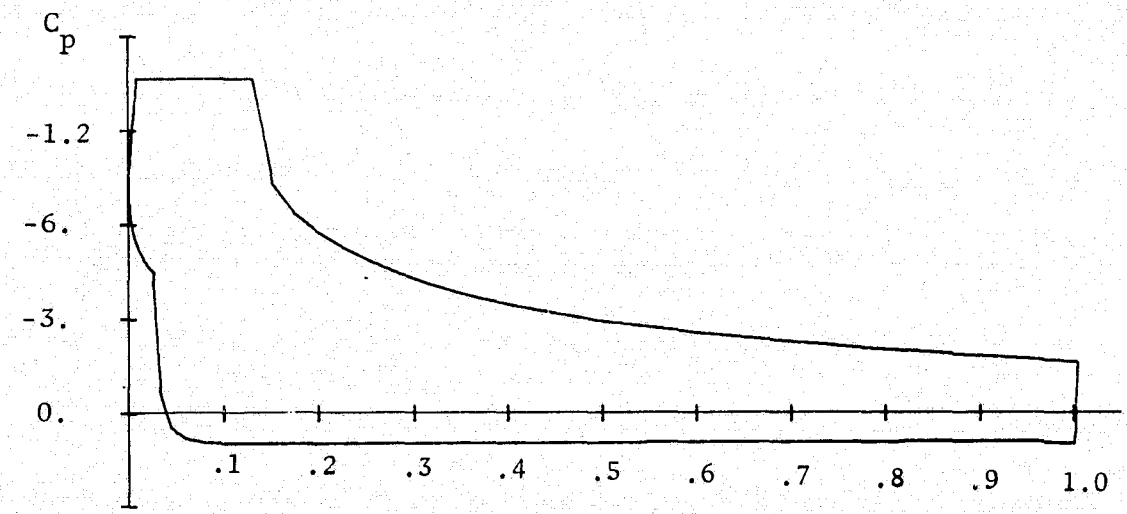

U of I HLE 1352-25-29-17

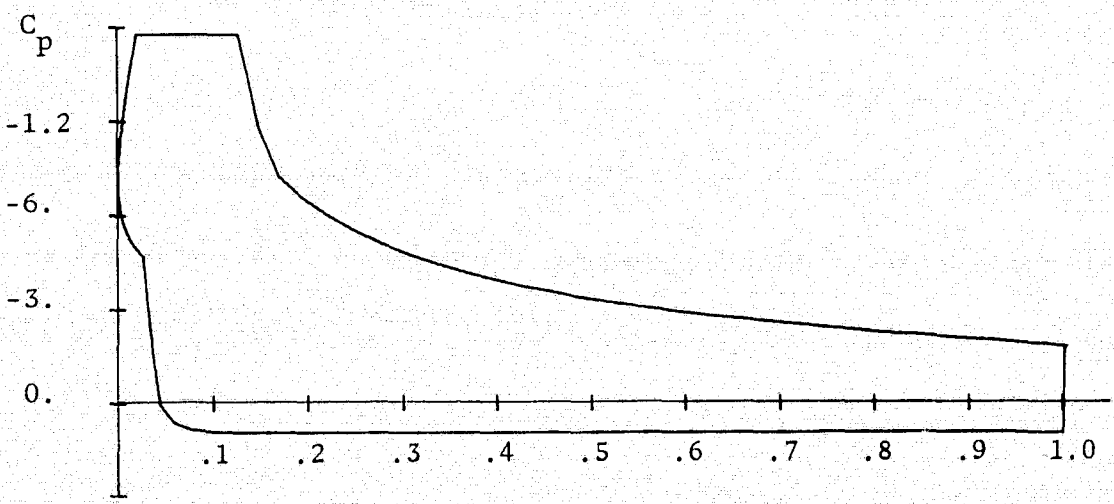

U of I HLE 2857-12-27-20

Figure 8. Several pressure distributions

V. SUGGESTIONS FOR FURTHER STUDY

There are several directions in which continued study of airfoils with a Stratford distribution could be channeled. Perhaps the most pressing is the matter of what trailing edge velocity to use. Conventional NACA series airfoils, as listed in Abbott and Von Doenhoff [13], have a trailing edge velocity in the neighborhood of $.8U_\infty$, which is significantly less than the values attained in the present study. While it is generally agreed that the trailing edge velocity of an airfoil must be limited, a cursory search of available literature has not indicated what the maximum value can be. Smith [14] demonstrates that increasing the trailing edge velocity will increase the lift, but indicates that the method of increasing the velocity above $.8U_\infty$ is through the use of flaps, and does not discuss the possibility of increasing trailing edge velocity through design of the airfoil. Edwards [5] indicated difficulty with the thickness of the airfoil and trailing edge shape when the trailing edge velocity exceeded 1.08. The trailing edge velocities of the airfoils in the present study are quite possibly too high, indicating that the separation of the trailing edge will move forward on the upper surface, destroying the pressure distribution. What needs to be done is, first, a systematic review of the literature to find if a maximum value of trailing edge velocity has been determined, and, second, if nothing is found in the literature, a maximum trailing edge velocity should be determined, either through experimental or analytical methods.

Another inconsistency in applying the Stratford distribution is in the determining of k. In equation (93) (for fully turbulent flow) or

equation (107) (for partially laminar flow), the assumption was made that $\frac{U}{U_0}$ was equal to one from the stagnation point to the point where the pressure rise began. In order to maximize the lift at design angle of attack, this is true. However, this implies that the stagnation is on the leading edge, which leads to a sharp leading edge. This sharp leading edge means a negative pressure peak at the leading edge in off-design conditions, which will result in separation of the boundary layer. What actually happens in the design of the airfoils is the stagnation point moves down on to the lower surface, and moves back towards the trailing edge some distance. For example, the stagnation point of the 1657-20-38-19 airfoil is at about $\frac{x}{c} = 0.18$. The velocity forward of the stagnation point remains at a low level until after the flow has gone around the leading edge, where it accelerates to the rooftop velocity. To correct for this error, the Stratford program should be rewritten, using equation(93) or equation (107) to define k.

As noted in chapter 4, a small protuberance is generated on the lower surface at the trailing edge, due to the large trailing edge angle. One method of eliminating this large trailing edge is to increase the length of the cusped region. This was done to the 1657-20-28-19 airfoil, with the resulting profile shown in figure 9 and the resulting pressure distribution shown in figure 10. The cusped region in this case was increased until the resulting x's in the airfoil profile were in monotonically increasing order on the upper surface. The resulting ϕ_s was 8.0 circle divisions, or 31.3°. It was necessary to adjust ϕ_w and ϕ_1 in order to match the Stratford distribution, but the remaining inputs are the same as the original airfoil. The resulting ϕ_w was 42.5, compared to

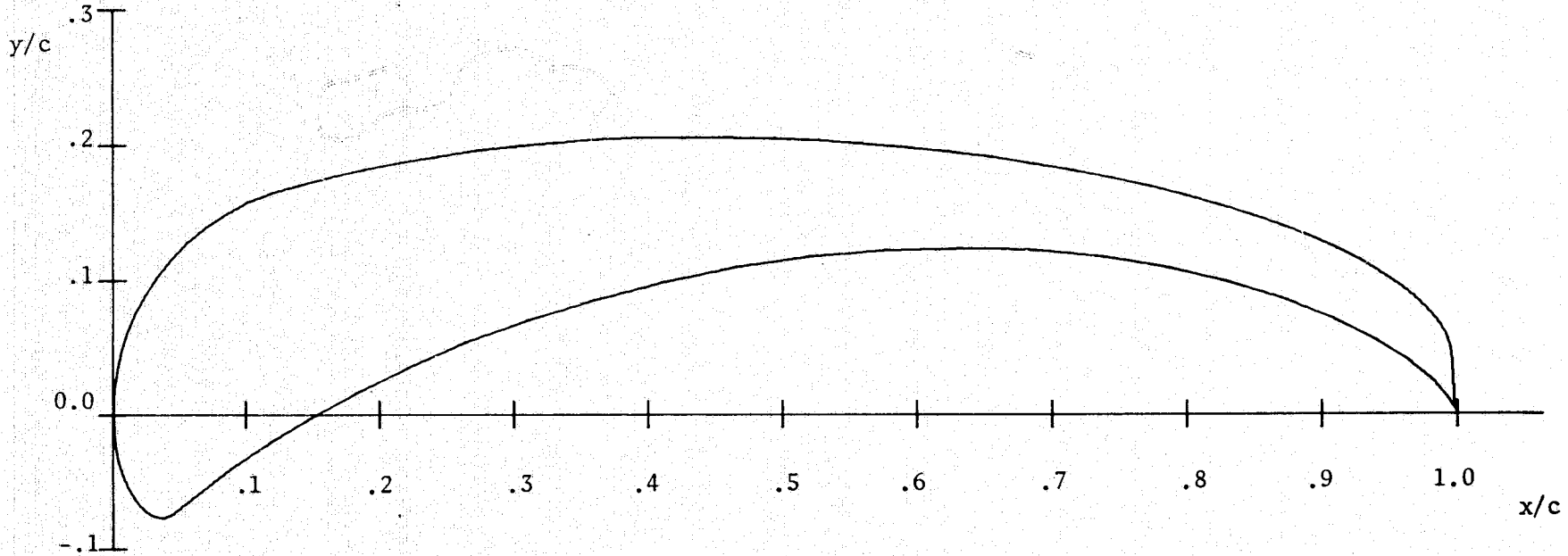

Figure 9. U of I HLE 1657-20-28-19 Airfoil (Modified trailing edge)

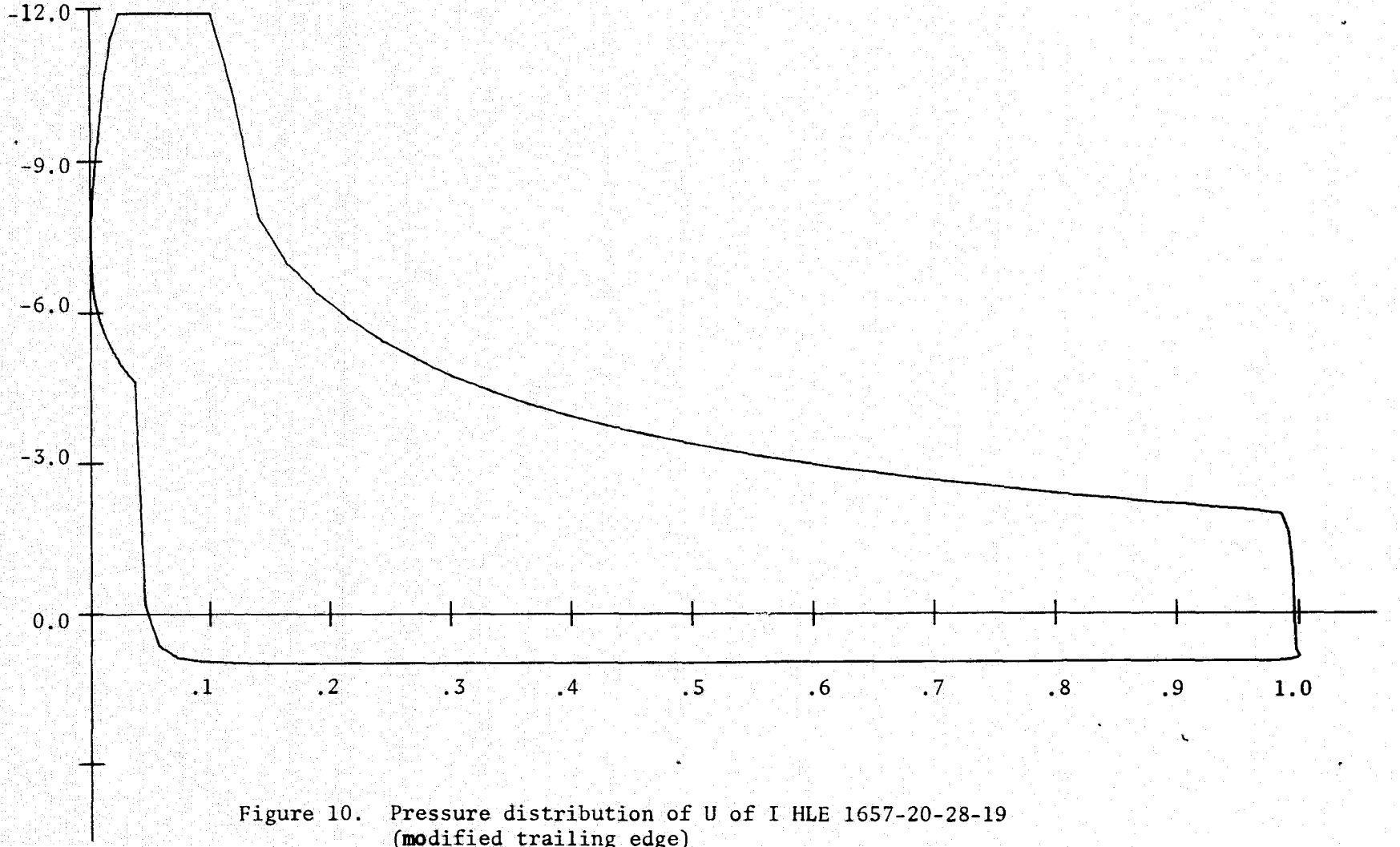

Figure 10. Pressure distribution of U of I HLE 1657-20-28-19 (modified trailing edge)

42.9 on the original airfoil, and the resulting ϕ_1 was 40.8, compared to 41.2. The geometric angle of attack changed to 22.69° from 19.06°. One unexpected improvement was the change in design lift coefficient predicted by the Lockheed program. The original airfoil had a design C_L of 3.868, while the airfoil with the modified trailing edge had a design C_L of 5.845

The concentration of the design of airfoils in the present study was on the upper surface. The α_i on the lower surface was the variable allowed to vary in the iteration to set $K_H + \overline{K}_H = K_s$. Perhaps one area of further study could be designing the lower surface such that a Stratford distribution occurs on the lower surface as well as on the upper surface. This would result in an airfoil with better off-design performance, as the flow would probably remain attached for all angles of attack between the design angle of attack on the upper surface and the design angle of attack on the lower surface. If the design angle of attack on the lower surface was the negative of the design angle of attack on the upper surface, and R_{e_0} was the same for both upper and lower surfaces, the resulting airfoil would be a symmetrical airfoil. This design of symmetrical airfoils suggests a further possible use of the program, the design of low drag struts. These low drag struts would simply be symmetrical airfoils, with $\alpha_i = \alpha_1 = 0.0$ (the design angle of attack) in the region $\phi_0 \leq \phi \leq \phi_1$, with $\phi_1 \geq \phi_w$. In the region $\phi_1 < \phi < \phi_{I_L}$, $\alpha_i = \alpha_2$ would be some positive angle of attack. As α_2 is increased, the thickness of the strut will increase. In order to get a true Stratford distribution, the modification redefining k described earlier would need to be implemented, as it is impossible to have another constant velocity on the upper and lower surfaces simultaneously.

to have a constant velocity on the upper and lower surfaces simultaneously.

Another improvement to the design method would be to combine the Eppler and Stratford program, so no visual comparison of the two velocity distributions would be necessary. This could be done by changing the form of W_w to be of the form

$$W_w = \left|1 - C_{p_0}\left(\frac{x}{x_0}\right)\right|^{1/2} \tag{122}$$

where $C_{p_0}\left(\frac{x}{x_0}\right)$ is given by equations (82) and (83). R_{e_0} would be an input parameter to the problem. Assuming $\phi_1 \geq \phi_w$, V_1 would then be equal to q_0, and the velocity would be of the form of equation (86). The form of W_s could remain as it is to allow control over the trailing edge angle. It might then be necessary to iterate on ϕ_w until equation (105) is satisfied in order to achieve a maximum lift.

One of the undesirable features of the airfoils designed in the present study is the large positive pitching moment. This moment might be reduced with a sacrifice of some lift by allowing the suction rise at the leading edge to occur more slowly. This would result in a less negative pressure region in the forward region of the upper surface, and thus a smaller moment. This slower suction rise could be input by specifying α_i to be greater than the design angle of attack in the region $\phi_w < \phi \leq \phi_{I_L}$. If k were modified as described earlier, the value of k would be increased by this slower suction rise (since $\frac{U}{U_0}$ would be less than one over much of the rooftop region), causing the start of the pressure rise region to move farther aft, regaining some of the lift lost by the loss of the low pressure region at the leading edge.

The airfoils of the present study were all designed with a critical Reynolds number of 3.2×10^5. However, data [15] from tests of the University of Illinois HL-1720-00 airfoil indicates the flow remains laminar throughout the rooftop region. The results of the Lockheed [12] program tend to support this result on the airfoils designed in the present study. Therefore, perhaps for future studies the critical Reynolds number should be defined by equation (116).

APPENDIX A

THE EPPLER PROGRAM

The calculations required for the solution of the Eppler problem are carried out with the aid of an IBM-360/75 computer at the University of Illinois. The Eppler program not only determines the profile of the airfoil but also determines the boundary layer momentum thickness and the energy form parameter. However, in the present application, the boundary layer capabilities of the program have not been fully utilized.

The required programs are kept in files on the PLORTS system. The file name of the Eppler program is EPPLER, while the file names of the required input data are EDATA through EDATG. A sample imput data deck is shown in Figure A1.

The first card in an input data deck for the Eppler program is a card with an Alpha-numeric listing of the titles of the cards that follow. These titles are read in 20A4 format. It is essential that the order of the titles not be changed and all titles must be included on this card, even if the named card is not used in the program. This first card can be thought of as part of the program itself, as it is never changed. The remaining cards, with the exception of the title, are in the format (A4,16,14F.2). Some of the data that is input through the F5.2 format is divided by a factor of 10 in the program, so it is important not to specify the decimal point. All the data should be right justified, and the program will convert the data to the correct multiple of 10. The data that is divided by 10. in the program will be identified in the following discussion as having a psuedo-format of F5.3.

The manner in which the data on each card is treated is determined by the title, which is listed in the first 4 spaces on each card. The

```
TRA1TRA2ALFAAGAMABSZ  REENDEBETAPLOTTITL
ABSZ           9200  100
AGAM            100  100    100    100   100   100
TITL
U OF I  HLE    1657-20-28-19       AIRFOIL
PLOT           3470-833721288156253307110894240000
TRA10000027    4120 4800 4290 0975 0000 4800 9200 3200
TRA2000027      150 4290  100 5000 0542  300 4000  100 8000 0499  20014500 001
BETA    -1      100
  RE       03       01633
ENDE
/*
```

Figure A1. A sample input data deck

data is read into the program as MARKE, NUPU, and PUFF, where MARKE is the title, NUPU is an integer, and PUFF is a 14 element array. The data is then transferred to the appropriate variable according to the title.

The first title listed on the first card is the TRA1 title. The TRA1 card is the card that inputs the ϕ_i and α_i. The ϕ_i are input in terms of circle divisions, and the ϕ_i are input in degrees. ϕ_{I_L} is determined by the program, so it is input as zero. The ϕ_i and α_i are input as pairs, and up to seven pairs can be input on one card. If it is desired to break the circle plane into more than seven segments, more TRA1 cards need be specified; with a maximum of four cards, as storage is allowed for only 28 segments. The last ϕ_i must be equal to the number of divisions in the circle. The ϕ_i must be listed in increasing order, including the computed value of ϕ_{I_L}.

Spaces 5 through 10 of the TRA1 card (NUPU) are reserved for the profile number. If several different airfoils are developed at the same time, they can be identified by this profile number.

Spaces 5 through 10 of the TRA2 card are also reserved for the profile number, but in this case, the profile number is used only to keep track of the input data, as this number is not used in the program. These spaces can also be left blank on the TRA2 card.

The remainder of the words on the TRA2 card define the input velocity function. Words 1 through 5 define the upper surface and words 6 through 10 define the lower surface. Word 1 is ϕ_s, given in circle divisions, and word 2 is ϕ_w. The meaning of words 4 and 5 depends on the word 3. If word 3 is 0.0, word 4 is k and word 5 is μ.

If word 3 is 1.0, word 4 is w' and word 5 is w. If word 3 is 2.0, word 4 is μ and word 5 is w. Words 4 and 5 are divided by 10.0 in the program, so the psuedo format is F5.3.

The specification of w and w' (word 3 being equal to 1.0) is recommended only with large values of w', so the path of W_w is strongly curved. The process converges slowly when w' is small, and convergence is not guaranteed when μ is negative. For less strongly curved paths, the specification of μ and w is recommended (word 3 equals 2.0).

Words 6 through 10 define the lower surface in the same manner that words 1 through 5 define the upper surface. Thus, for a symmetrical airfoil, words 6 through 10 would repeat words 1 through 5.

Word 11 is referred to as ITMOD, and determines the variable that is changed in the iteration process to set K_s to the specified value. The ITMOD is 0.0, no iteration is carried out. If ITMOD is 1.0, the α_i on the upper surface are altered by a factor $\Delta\alpha_i$ until K_s attains the desired value. If ITMOD is 2.0, the α_i the lower surface will be altered and if ITMOD is 3.0, the α_i will be altered on both the upper and lower surface by an equal amount. If ITMOD is 4.0, K is modified, if ITMOD is 5.0, $\overline{K}$ is modified, and if ITMOD is 6.0, K and $\overline{K}$ are modified by equal amounts. ITMOD = 3.0 or 6.0 is useful for symmetrical airfoils.

Word 12 is K_s, written in the psuedo-format of F5.3. Word 13 is the tolerance acceptable in the K_s computation, also written in the pseudo-format of F5.3. A suggested value for this is .001, the smallest value available in the F5.3 format. Word 14 is not used.

The next card in the list is the ALFA card. This card inputs the various angles of attack that the pressure distribution is developed for

and that are used in the boundary layer portion of the program. The first word after the title is NAL, the number of angles of attack listed, in I6 format. NAL can be as large as 14. If NAL is specified as larger than 14, it is reset to 4. The next 14 (or less) words are the angles of attack, in degrees, written in F5.2 format. If NAL is given as a negative number, the angle of attack will be α_i given on the TRA1 card, where i is on the ALFA card in F5.2 format (see the sample data deck in Figure A1 for an example of this) If an ALFA card is given with no angles of attack and NAL=0, the angles of attack of the previous profile are repeated.

The AGAM card controls the output of the Eppler program. The I6 of the AGAM card is ignored, but 14 AGAM(i)'s are read in F5.2 format. In general, the AGAM(i)'s are either zero and not zero. If AGAM(1) is not zero, the x and y coordinates of the airfoil are generated. If AGAM(1) is equal to zero, only the transcendental equation is solved. If AGAM(2) is not equal to zero, the profile list will be printed, along with a velocity distribution for each angle of attack on the ALFA card. If AGAM(3) is not zero, the input data and the solution to the transcendental equation is printed out for the initial input and the final iteration. If AGAM(4) is not zero, the input data and the solution to the transcendental equation will be printed out for all iterations. AGAM(5) and AGAM(6) refer to the boundary layer portion of the program. If AGAM(5) is not zero, the program will print out a listing of the distance along the surface from the stagnation point, the local velocity, the energy thickness form parameter H_{32} (the energy dissipation boundary layer thickness divided by the momentum thickness), and the momentum thickness. If AGAM(5) is equal to 1.0, the local Reynolds number, based on the momentum thickness and the local velocity is printed out instead of the momentum thickness. If AGAM(6)

is not equal to zero, the boundary layer transition point, boundary layer separation point, and drag (calculated by the Squire Young Method) are printed out. AGAM(7) through AGAM(14) are not presently used, but are reserved for further use.

At the University of Illinois, most runs are made with AGAM(1) through AGAM(6) equal to 1.0. This results in the most complete output. An attempt to run with AGAM(6) equal to zero resulted in the failure of the program for unknown reasons.

Card ABSZ lists the number of circle divisions, NKR, in spaces 11 through 15. NKR must be divisible by 4, and NKR + 1 points result in the profile of the airfoil. As NKR is increased, the accuracy of the solution increases, as well as the computational time required. The maximum NKR is 120, but 60 is usually a sufficient number unless large slopes in the velocity function are encountered, as with a Stratford distribution. For the airfoils designed at the University of Illinois, an NKR of 92 was chosen.

The ABSZ card also lists ABFA in spaces 16 through 20, which multiplies all values given in circle divisions. ABFA is normally equal to 1.0. It is necessary to change ABFA only if the number of circle divisions is changed, so it is not necessary to change all the input data given in circle divisions. If no ABSZ card is given, NKR is set to 60 and ABFA is set to 1.0.

The RE card is used to input the Reynolds number into the program. The pseudo-format of the RE card is (A4, 6X, 5(2I1, 3X, F5.3)). The first of the I1 words represents MA, which at one time was used to determine the suction mode. Since the capability of boundary layer suction has been removed from the program, this word is no longer used. The second I1 word is MU, the mode for boundary layer transition. When MU is equal to 1,

transition is by laminar separation. If MU is equal to 2, transition occurs at the first decrease in velocity. If MU is equal to 3, transition occurs when the velocity remains constant throughout a step distance or decreases. If MU is 4, transition occurs when the natural logarithm of the local Reynolds number based on δ_2 and the local velocity exceeds or equals $18.43\ H_{32} - 21.74$. MU = 5 is similar to MU = 4, except the value that ln (RE) is compared to is $18.43\ H_{32} - 22.10$. Therefore, MU = 5 is a more conservative estimate for transition. The F5.3 word is the free stream Reynolds number, based on the chord length and free stream velocity. All lengths in the program are non-dimensionalized with respect to this chord length, and all velocities are non-dimensionalized with respect to this velocity. There can be up to 5 Reynolds numbers, each with its own MA and MU. The program will continue to read in Reynolds numbers (up to 5) until a zero value is read as a Reynolds number.

The ENDE card is necessary for proper termination of the program. It is the final data card, and indicates all data has been read in.

The next three titles on the list are cards that have been added to the program at the University of Illinois. The first of these cards is the BETA card, which replaces the ALFA card. If a BETA card is used instead of an ALFA card, either a punched output is generated or data is filed into the PLORTS system that is used by the Stratford program. This data consists of four parts, written in 6F12.9 format. The first part is DS, the increment of the surface distance for each x increment. There are NKR DS's generated. The other three parts are a velocity function (VF), and x and y coordinates of the airfoil. There are NKR + 1 of each of these values. The velocity function is equal to the local velocity divided by $(1 + \cos\alpha_i)$.

The program was originally designed to give a punched output, but was modified to file the data directly into PLORTS. However, as the PLORTS system is due to be removed from the IBM-360 at the University of Illinois, it will be necessary to change back to a punched output deck.

The next card that has been added to the program is the PLOT card. This card reads data into the system that is then either punched out or filed into PLORTS. Nothing is done with this data by the program, as this is only a convenient method of getting data into the input deck for the Stratford programs.

The last card to be described is the TITL card. No data is on the TITL card, but this card signals that the next card is in 20A4 format, and is the title of the airfoil. This title will be printed in the output and inserted into the Stratford input deck.

There are some restrictions on the order the cards are read in. The ABSZ (if one is used), AGAM, TITL, and PLOT cards should be read into the computer first, although not necessarily in that order. The data on these cards remains valid until another similar card is read into the computer. Thus, for example, if several profiles are to be developed with the same number of circle divisions, it is not necessary to repeat the ABSZ card. The next cards to be read in are the TRA1 and TRA2 cards, in that order. Once the TRA2 card is read in, the profile is generated. The ALFA or BETA card is then read in, followed by the RE card. The RE card initiates the calculation of the boundary layer. If other profiles are desired, new TRA1 and TRA2 cards can now be read in, preceded by new ABSZ, AGAM, PLOT, and TITL cards, as necessary. These cards can be followed by ALFA or BETA and RE cards if boundary layer information is desired.

The ENDE card terminates the program after all the profiles and boundary layer calculations are complete.

The descriptions of the output which follows assumes AGAM(1) through AGAM(6) are not equal to zero. If any of these words are equal to zero, the corresponding portion of the output will be deleted.

The first data listed in the output are the input data and the solution to the transcendental equation. This data is preceded by the title, profile number, iteration number, and iteration mode (0 through 6). The headings of the table of data do not agree with the nomenclature presented in this paper. NUE represents the same quantity as ϕ_i, ALPHA is α_i, WS is w and $\overline{w}$, WHK is w' and $\overline{w}'$, DRAK is K and $\overline{K}$, DRAM is μ and $\overline{\mu}$, HK is K_H and $\overline{K}_H$, FLA is ϕ_w and $\overline{\phi}_w$, and LAS is ϕ_s and $\overline{\phi}_s$.

The next data listed are the profile of the airfoil in x and y coordinates and the velocity distribution for each angle of attack on the ALFA or BETA card. AT the end of this listing, the values of CM, BETA, ETA, SX, and SY are printed out. CM is the moment coefficient at zero lift and BETA is the angle between the zero lift line and the chord line. Since all angles of attack are given in reference to the zero lift line, this angle is necessary to compute the geometric angle of attack. ETA, SX, and SY are apparently remnants of trouble shooting the program, as they are not particularly useful. ETA is the number of points in the circle plane divided by the chord and π. This term is used in non-dimensionalizing the chord. SX and SY are summation of the x and y coordinates of the airfoil profile.

The last section of data is derived from the boundary layer portion of the program. First there are two tables, one for the upper surface and

one for the lower surface. These tables list the surface coordinate, local velocity, H_{32}, and δ_2. If AGAM(5) is equal to 1.0, the local Reynolds number based on δ_2 and the local velocity is printed in place of δ_2. However, nothing in the output indicates that this has been done, so it is important that it be noted that AGAM(5) is equal to 1.0 if this data is to be used. If H_{32} is a negative number, the flow in the boundary layer is turbulent.

Following these two tables are listings for the upper and lower surface transition points, separation points, and drag coefficients. Once again, there is a problem of nomenclature, as the transition points are under the heading INS., the separation points are under the heading TRANS., and the drag coefficient are under the heading SEP.. The transition and separation points are given in terms of surface coordinates.

The plotting routine for the Eppler airfoils is filed in two PLORTS files, PLOTMN and PLOTOBJ. The data for the plotting routine is normally filed in PLDAT(N) and PLOTOBJ(N), where (N) is a number between 1 and 5. The first card in PLDAT(N) is a card of the form b&NAMlbN=92,ALPHA=18.42,&END where b is a blank space, N is the number of points on the airfoil (normally 92), and ALPHA is the design angle of attack. This card is a punched output card of the Eppler program, but it is not the first card. Therefore, the deck must be rearranged to be in the proper order. The next part of the PLDAT(N) file consists of the DS, VF, x, and y cards, as punched out by the Eppler program. Finally, the first card is repeated four times, but with different angles of attack. The only data that is changed in the PLOTOBJ(N) file is the first card, which is the title card in 20A4 format. The

remainder of the data in the PLOTOBJ(N) file is concerned with numbering the axis, and always remains the same.

The plotting files are run in the following order: PLOTMN, PLDAT(N), PLOTOBJ, PLOTOBJ(N). The first (or main) portion of the program (that part filed under the PLORTS file PLOTMN) determines the pressure coefficients, circulation, lift coefficient, and center of circulation, first for the design angle of attack and then for the other four angles of attack listed on the last four cards in PLDAT(N). The airfoil coordinates and pressure coefficients are stored on tape. The second part of the program (PLOTOBJ) then runs, reads the data on tape, and plots the airfoil profile and pressure distribution for the design angle of attack.

APPENDIX B

THE STRATFORD PROGRAM

The Stratford program is divided into two parts. The first part, which is kept in the PLORTS file TABLE, determines the roots of equation (117). The second part, kept in the PLORTS file STRPLOT, takes the output data from TABLE and the Eppler program and plots a Stratford distribution that corresponds to the RE0 input to TABLE with an initial velocity equal to the rooftop velocity of the Eppler airfoil.

There is no external input data for the program in the file TABLE. If a different set of data is desired, the changes have to be made in the program itself. Therefore, for example, the statement RECR = N.NEN, where N.NEN is the desired critical Reynolds number, must appear early in the program. The program is set up to solve equation (117) for up to 30 values of R_{e_0}. If less than 30 values are desired, the statement NUM=30 must be altered to reflect this. The first value of R_{e_0} is input through the statement RE0(1)=N.NEN, where N.NEN is the desired value. The remaining values of R_{e_0} are input through the statement RE0(K+1)= RE0(K)+N.NEN, where N.NEN is the desired step size. The trailing edge velocity can be input through the statement VTE=NN.N, but, since all the data except x_0 and the chord length are non-dimensionalized, this value is of no consequence. If a value of kinematic viscosity (ν) other than 1.6×10^{-4} is desired, the statement ANU=160.E-6 can be changed to reflect this.

The roots of equation (117) are determined through the use of a subroutine from the IBM Scientific Subroutine Package [17] named POLRT.

This subroutine determines all of the roots of the polynomial, and the program searches through these roots until it finds the positive real root. From this real root, the value of Z can be determined. Through the use of equation (101), the ratio of q_u/q_0 can then be determined, and, from equation (106), the value of x_0 can be determined.

For each value of R_{e_0}, the TABLE program prints out values of k, a', b', D = q_u/q_{Ie}, Z, z_m, x_0, and the chord length. The values of a', b', D, z_m, Z, k, and R_{e_0} are read into the Eppler program through the PLOT card, and are then output with the rest of the Eppler output either on cards or filed into PLORTS. This data is used by the second part of the Stratford program, which is filed in the PLORTS file STRPLOT.

The program in STRPLOT takes the data from the Eppler program, and, through the use of the Calcomp plotter, draws the required Stratford pressure distribution based on the data from TABLE and the Eppler program. The first card read into STRPLOT is the title, written in 20A4 format. The second card contains N, SF1, and SF2, in I4, 2F10.7 format. N is a number that is no longer used in the Stratford program, and can be left blank. SF1 is a scale factor in the x direction. In order to match the output of the Eppler plot program, this should be 10.0. SF2 is the scale factor in the y direction, and should be 0.3125 to match the Eppler plot. The next data read in are a', b', D, U_0, z_m, Z, s_u, and k, in 8F10.7 R_{e_0} is then read in F15.4 format. The last two sets of data read in are the x coordinates of the airfoil and DS, the surface distance between the points on the airfoil. Both of these sets of data are in 6F12.9 format. The program is presently set up for 93 points on the airfoil.

The chord Reynolds number is calculated by the formula

$$R_{e_c} = \frac{R_{e_0}}{U_0 x_0 s_u} \tag{B1}$$

and printed in the output.

APPENDIX C

THE LOCKHEED PROGRAM

The Lockheed program was used as a method of checking the results of the Eppler program. Given the coordinates of an airfoil, the Lockheed program determines the lift, drag, and moment coefficients. The theory and application of the Lockheed program is documented in references 12 and 17. However, there have been a few modifications to the program as run at the University of Illinois. These modifications will be the subject of this appendix.

The input cards to the program are the same as in reference 12 except for cards 2 and 3. Card 2, which is concerned with the plot subroutine that is not used, was eliminated. Card 3 has two more variables, IPLOT and MXTRAP. IPLOT is presently not used, but is reserved for use in conjunction with a plotting subroutine. MXTRAP will be explained in the following pages.

The major modification to the program was the restoration of the smoothing process of the local Mach number at the trailing edge. As noted in reference 18, large Mach number gradients at the trailing edge create undesired "kinks" in the equivalent airfoil camber line. In order to correct for this, the computed Mach numbers at the last two points on the upper surface of the airfoil are discarded, and a linear least-squares fit is applied to the last five remaining points on the upper surface. The least squares fit is then shifted until a smooth transition occurs at the most forward point (i.e., at the seventh point from the trailing edge), and the curve is extrapolated to replace the last two points. The computed Mach number at the last three points on the lower surface is then discarded, and a second order interpolation between the last point on the upper surface and the

fourth and fifth points from the trailing edge on the lower surface is used to redefine the last three points on the lower surface. These modified values of local Mach numbers are used only to determine the local boundary layer characteristics. The actual computed values are printed out in the output of the Lockheed program.

When North Carolina State University modified the multi-element program to obtain the single element program described in reference 12, they found that the smoothing and extrapolation resulted in a significant lift from symmetrical airfoils at zero angle of attack. Therefore, they removed this portion of the program. Studies at the University of Illinois have shown that correlation with analytical results (at least for airfoils with a Stratford distribution) is better with the smoothing and extrapolation routine in the program. Therefore, the smoothing and extrapolation routine was restored, but with two modifications. First, a second order least squares fit was used on the upper surface, and, second, the number of points smoothed on the upper surface was made a variable called MXTRAP. If MXTRAP is 0, no smoothing is done, while if MXTRAP is a positive integer greater than 2, this number of points are smoothed on the upper surface. MXTRAP should be at least 3 so a second order least square fit can be done. Most of the work at the University of Illinois has been done with MXTRAP=7, so the smoothing routine is the same as the original multi-element Lockheed program.

For each angle of attack, the resulting lift coefficient is divided by the drag coefficient. This lift over drag data is then printed out in the table at the end of the output, along with the lift, drag, and moment coefficients.

The punch option was modified to make it compatible with the plotting routine at the University of Illinois. The first punched output card is the title, in 20A4 format. The next card contains the reference chord length, stagnation temperature, chord Reynolds number, Prandtl number, heat transfer coefficient, MXTRAP, and the number 1 in (5F12.5,2I5) format. This last number 1 indicates to the plotting routine that the single element program was used, as opposed to the multi-element program. The third card contains the number of elements in the airfoil (always one) and the number of points in the airfoil (always 65) in 2I5 format. The fourth card lists the number of free stream Mach numbers and the number of angles of attack in 2I5 format. The next sets of data are the x and y coordinates of the airfoil in 6F12.8 format.

The remaining data is repeated for each angle of attack and each Mach number. The first two cards list the separation points for the upper and lower surface. Often, due to an unknown problem in the program, an extra card is punched out at this point, indicating no transition on either the upper or lower surface. Therefore, before the output deck can be used, it must be checked to make sure there are only two cards listing separation points for each angle of attack and Mach number combination. The next card lists the free stream Mach number and angle of attack in 2F12.5 format. This is followed by the lift coefficient, drag coefficient, and moment coefficient in 3F12.5 format. The last portion of data is the local pressure coefficient at each of the 65 points on the airfoil in 6F12.8 format.

This punched output is then fed into the plotting program, which is filed in PLORTS under the file name PICT. This program plots (using the calcomp plotter), first, an outline of the airfoil profile, with a listing

of the reference chord length, stagnation temperature, chord Reynolds number, Prandtl number, and heat transfer coefficient. The program then plots a pressure distribution for each angle of attack and Mach number. If at least three angles of attack have been specified, the program then plots a C_L versus angle of attack curve, a C_D versus C_L curve, and a C_m versus C_L curve. If the boundary layer separates at some point before $x/c = 0.95$, the point of separation is indicated on the C_L versus angle of attack curve.

LIST OF REFERENCES

1. Liebeck, R. H., "Optimization of Airfoils for Maximum Lift," Ph.D. Thesis, University of Illinois, Urbana, 1968.

2. Ormsbee, A. I., and Chen, A. W., "Multiple Element Airfoils Optimized for Maximum Life Coefficients," Journal of Aircraft, Vol. 10, No. 12, December, 1972, pp. 1620-1624.

3. Chen, A. W., "The Determination of the Geometries of Multiple Element Airfoils Optimized for Maximum Life Coefficients," Ph.D. Thesis, University of Illinois, Urbana, 1968.

4. Awker, R. W., "The Design and Test of a Single Element Airfoil Optimized for High Lift," M.S. Thesis, University of Illinois, Urbana, 1974.

5. Edwards, T. E., "On Perturbation Solutions for the Laminar Incompressible Boundary Layer with Variable Mass Transfer at the Wall," Ph.D. Thesis, University of Illinois, Urbana, 1966.

6. Stratford, B. S., "The Prediction of Separation of the Turbulent Boundary Layer," Journal of Fluid Mechanics, Vol. 5, 1959.

7. Eppler, R., "Direkte Berechnung von Traflügelprofilen aus der Druckverteilung," Ingenieur-Archiv, Vol. 25, 1957, pp. 32-57.

8. Miley, S. J., "An Analysis of the Design of Airfoil Sections for Low Reynolds numbers," Ph.D. Thesis, Mississippi State College, 1972.

9. Wortmann, F. X., "Ein Beitrag zum Eniwurg von Laminar Profilen fur Segelflugzeuge und Hubschrauber," Zeitshrift Fur Flugwissenshaften, October, 1955.

10. Stratford, B. S., "An Experimental Flow with Zero Skin Friction Throughout It's Region of Pressure Rise," Journal of Fluid Mechanics, Vol. 5, 1959.

11. Schlichting, H., "Boundary-Layer Theory," Sixth Edition, McGraw-Hill, New York, 1968.

12. "Program for the Calculation of Two Dimensional Aerodynamic Characteristics," Unpublished NASA-LRC Report.

13. Abbott, I. H., and Doenhoff, A. E., "Theory of Wing Sections," Dover Publications, New York, 1949.

14. Smith, A.M.O., Fluid Dynamics of Airfoil Stalling," AGARD Conference Preprint No. 102, April 1972.

15. Wortmann, F. X., Private correspondence with A. I. Ormsbee, 1975.

16. Eppler, R., "Praktische Berechnung Laminarer und Turbulenter," Ingenieur-Archiv, Vol. 32, 1963, pp. 221-245.

17. System/360 Scientific Subroutine Package, Version III, programmers manual, fifth edition, International Business Machine Corp., White Plains, New York, August 1970.

18. Stevens, W. A., Goradia, S. H., and Braden, J. A., "Mathematical Model for Two-Dimensional Multi-Component Airfoils in Viscous Flows," NASA CR-1843.

UNIVERSITY OF ILLINOIS

RECENT AERONAUTICAL AND ASTRONAUTICAL
ENGINEERING DEPARTMENT TECHNICAL REPORTS

Technical Report Number	Title	Author	Journal Publication
AAE 62-1	An Introduction to Viscoelastic Analysis	H. H. Hilton	Engineering Design for Plastics, Reinhold Publ. Corp., N.Y., 199-276 (1964).
AAE 62-2	A Method of Characteristics Analysis of Detonation Stability	R. A. Strehlow	
AAE 63-1	On Non-Stationary White Noise	Y. K. Lin	J. Acoust. Soc. Amer. 36:82-84 (1964).
AAE 63-2	Formulation and Evaluation of Approximate Analogies for Transient Temperature Dependent Linear Viscoelastic Media	H. H. Hilton and J. R. Clements	Proc. Conf. on Thermal Loading and Creep, Inst. Mech. Eng., London, 6.17-6.24(1964)
AAE 63-3	Free Vibrations of Continuous Skin-Stringer Panels with Non-Uniform Stringer Spacing and Panel Thickness	Y. K. Lin, T. J. McDaniel, B. K. Donaldson, C. F. Vail and W. J. Dwyer	AFML-TR-64-347, Wright-Patterson AFB (1965)
AAE 64-1	Random Vibrations of a Myklestad Beam	Y. K. Lin	AIAA J., 2:1448-1451 (1964)
AAE 64-2	On Detonation Initiation	R. A. Strehlow	AIAA J., 2:783-784 (1964)
AAE 64-3	A Theoretical Investigation of a Restrictive Model for Detonation Initiation	R. B. Gilbert	AIAA J., 4:1777-1783 (1966)

RECENT AERONAUTICAL AND ASTRONAUTICAL ENGINEERING DEPARTMENT TECHNICAL REPORTS (continued)

Technical Report Number	Title	Author	Journal Publication
AAE 64-4	Transfer Matrix Representation of Flexible Airplanes in Gust Response Study	Y. K. Lin	J. of Aircraft, 2:116-121 (1965)
AAE 64-5	Dynamic Characteristics of Continuous Skin-Stringer Panels	Y. K. Lin	Acoustical Fatigue in Aerospace Structures, Syracuse Univ. Press, 163-184 (1965)
AAE 64-6	Experimental Study of the Growth of Transverse Waves in Detonations	R. Liaugminas	See AAE 66-3
AAE 64-7	Nonstationary Excitation and Response in Linear Systems Treated as Sequences of Random Pulses	Y. K. Lin	Journal of the Acoustical Society of America, 38: 453-460 (1965)
AAE 65-1	Transverse Waves in Detonations	R. A. Strehlow and F. Dan Fernandes	Combustion and Flame, 9:109-119 (1965)
AAE 65-2	A Summary of Linear Viscoelastic Stress Analysis	H. H. Hilton	Solid Rocket Structural Integrity Abstracts, 2: 1-56 (1965)
AAE 65-3	Approximate Correlation Function and Spectral Density of the Random Vibration of an Oscillator with Non-Linear Damping	Y. K. Lin	AFMK-TR-66-62, Wright Patterson AFB (1966)
AAE 65-4	Investigation of the Flow Properties Downstream of a Shock Wave Propagating into a Convergent Duct	R. E. Cusey	See AAE 65-6

RECENT AERONAUTICAL AND ASTRONAUTICAL ENGINEERING DEPARTMENT TECHNICAL REPORTS (continued)

Technical Report Number	Title	Author	Journal Publication
AAE 65-5	A Method for the Determination of the Matrix of Impulse Response Functions with Special Reference to Applications in Random Vibration Problems	Y. K. Lin	AFFDL-TR-66-80, Wright Patterson AFB, 743-751 (1966)
AAE 65-6	Convergent Channel Shock Tube for Detonation Initiation Studies	A. J. Crooker	"Detonation and Initiation Behind an Accelerating Shock Wave" by R. A. Strehlow, A. J. Crooker, R. E. Cusey, Comb and Flame, 11:339-351 (1967)
AAE 66-1	A Comparison of Experimental and Theoretical Transverse Wave Spacings in Detonation	R. H. Watson	See AAE 66-3
AAE 66-2	A Simple Model for the Mechanism of Detonation	J. R. Eyman	See AAE 66-3
AAE 66-3	Transverse Wave Structure in Detonations	R. A. Strehlow, R. Liaugminas, R. H. Watson and J. R. Eyman	11th Symposium (International) on Combustion, Mono Book Corp. Baltimore, Md., (1967)
AAE 66-4	A Real Gas Analysis Using an Acoustic Model for the Transverse Wave Spacing in Detonations	R. E. Maurer	AIAA Journal, 7: 323-328, (1969)
AAE 67-1	Shock Tube Studies in Exothermic Systems	R. A. Strehlow	Phys. Fluids, 12: 96-100, (1969).

RECENT AERONAUTICAL AND ASTRONAUTICAL ENGINEERING DEPARTMENT TECHNICAL REPORTS (continued)

Technical Report Number	Title	Author	Journal Publication
AAE 67-2	Shock Tube Chemistry	R. A. Strehlow	Progress in High Temperature Physics and Chemistry, Pergamon Press, N.Y., 2: 127-176 (1968).
AAE 67-3	Structural Failure Criteria for Solid Propellants Under Multiaxial Stresses	A. R. Zak	J. Spacecraft, 5: 265-269 (1968)
AAE 67-4	Structural Analysis of Realistic Solid Propellant Materials	A. R. Zak	J. Spacecraft, 5: 270-275 (1968).
AAE 67-5	Characteristics of Transverse Waves in Detonations of H_2, C_2H_2, C_2H_4 and CH_4 - Oxygen Mixtures	C. D. Engel	AIAA Journal, 7: 492-496 (1969).
AAE 68-1	A Review of Shock Tube Chemistry	R. A. Strehlow	Progress in High Temperature Physics and Chemistry, Pergamon Press, N.Y., 2: 1-146 (1969).
AAE 68-2	On the Interpretation of Molecular Beam Data	A. Klavins	A. Klavins and L. H. Sentman Rev. Sci. Instr., 41: 1560-1567 (1970).
AAE 68-3	Detonative Mach Stems	R. A. Strehlow H. O. Barthel	
AAE 68-4	On the Strength of Transverse Waves and Geometrical Detonation Cell Model for Gas Phase Detonations	J. R. Biller	R. A. Strehlow and J. R. Biller Comb. and Flame, 13: 577-582, (1970).
AAE 68-5	The MISTRESS User Manual	H. H. Hilton	
AAE 69-1	The Chemical Shock Tube - Implications of Flow Non-Idealities	R. A. Strehlow R. L. Belford	

RECENT AERONAUTICAL AND ASTRONAUTICAL ENGINEERING DEPARTMENT TECHNICAL REPORTS (continued)

Technical Report Number	Title	Author	Journal Publication
AAE 69-2	Phenomenological Investigation of Low Mode Marginal Planar Detonations	A. J. Crooker	Astronautica Acta (in press, 1974)
AAE 69-3	Multi-Dimensional Detonation Wave Structure	R. A. Strehlow	Astronautica Acta, 15:345-358(1970)
AAE 69-4	An Experimental and Analytical Investigation of a Two-Dimensionally Stiffened Panel	A. R. Zak C. E. French	AFML-TR-68-390, Wright-Patterson AFB, (1969)
AAE 69-5	On the Kinetic Equations for a Dilute, Short Range Gas	T. J. Forster L. H. Sentman	
AAE 69-6	The Sawtooth Column of the Supersonic Electric Arc in Sulfur Hexafluoride	C. E. Bond	AIAA J., 9: 510-512 (1971)
AAE 69-7	Theoretical and Experimental Analysis of Stiffened Panels Under Dynamic Conditions	A. R. Zak R. N. Yurkovich J. H. Schmidt	J. of Aircraft, 3: 149-155 (1971)
AAE 70-1	On the Interaction Between Chemical Kinetics and Gas-Dynamics in the Flow Behind a Cylindrical Detonation Front	S. Rajan	
AAE 70-2	Preliminary Studies on the Engineering Applications of Finite Difference Solutions of the Navier-Stokes Equations	W. F. Van Tassell	
AAE 70-3	Some Aspects of the Surface Boundary Condition in Kinetic Theory	A. Klavins	Proc. of International Symposium on Rarefied Gas Dynamics, Pisa, Italy (1970)

RECENT AERONAUTICAL AND ASTRONAUTICAL ENGINEERING DEPARTMENT TECHNICAL REPORTS (continued)

Technical Report Number	Title	Author	Journal Publication
AAE 70-4	A Study of the Transient Behavior of Fuel Droplets during Combustion: Theoretical Considerations for Aerodynamic Stripping	H. Krier	
AAE 70-5	On the Solid Body Model for an Accelerating Electric Arc	F. Klett	
AAE 71-1 UILU-ENG 71 0501	Detonation Mach Stems	R. A. Strehlow H. O. Barthel	
AAE 71-2 UILU-ENG 71 0502	An Investigation of Transient Phenomena in Detonations	R. J. Stiles	with R. A. Strehlow, A. A. Adamczyk, Astronautical Acta, 17, 509-527 (1972)
AAE 71-3 UILU-ENG 71 0503	On the Role of Tangential Velocity Changes in the Scattering of a Molecular Beam from A Solid Surface	C. C. Chrisman L. H. Sentman	
AAE 72-1 UILU-ENG 72 0501	Unconfined Vapor Cloud Explosions - An Overview	R. A. Strehlow	Fourteenth Symposium on Combustion, 1189-1200 (1973)
AAE 72-2 UILU-ENG 72 0502	Application of Illiac IV Computer to Numerical Solutions of Structural Problems	H. H. Hilton A. R. Zak J. J. Kessler P. C. Rockenbach	
AAE 72-3 UILU-ENG 72 0503	On the Measurement of Energy Release Rates In Vapor Cloud Explosions	R. A. Strehlow L. D. Savage G. M. Vance	Combustion Science and Technology, 6, 307-312 (1972)

RECENT AERONAUTICAL AND ASTRONAUTICAL ENGINEERING DEPARTMENT TECHNICAL REPORTS (continued)

Technical Report Number	Title	Author	Journal Publication
AAE 72-4 UILU-ENG 72 0504	A Performance Comparison of Several Numerical Minimization Algorithms	J. E. Prussing	
AAE 73-1 UILU-ENG 73 0501	Stresses and Damping in the Matrix of a Composite Material	A. R. Zak	
AAE 73-2 UILU-ENG 73 0502	Early Burning Anomalies in the XM 645 Flechette Cartridge	H. Krier D. R. Hall	BRL Rept. No. 104 (1973)
AAE 73-3 UILU-ENG 73 0503	Equivalent Explosive Yield of the Explosion in the Alton Southern Gateway Yard, East St. Louis, Ill., January 22, 1972	R. A. Strehlow	
AAE 73-4 UILU-ENG 73 0504	Failure Studies of Gaseous Detonations	R. J. Salm	
AAE 73-5 UILU-ENG 73 0505	An Investigation of Hydrogen-Oxygen-Argon Detonations	J. R. Biller	
AAE 73-6 UILU-ENG 73 0506	Interior Ballistic Predictions Using Data From Closed and Variable-Volume Simulators	H. Krier S. A. Shimpi M. J. Adams	
AAE 73-7 UILU-ENG 73 0507	Theory of Rotationally Symmetric Laminar Premixed Flames	G. M. Vance H. Krier	Comb. and Flame J., 22, 365-375 (1974).
AAE 73-8 UILU-ENG 73 0508	Burning of Fuel Droplets at Elevated Pressures	J. H. Rush H. Krier	Comb. and Flame J., 22, 377-382 (1974).
AAE 73-9 UILU-ENG 73 0509	An Impact Ignition Model for Solid Propellants	H. Krier H. H. Hilton O. Olorunsola D. L. Reuss	BRL Rept. No. 1707 (1974)

RECENT AERONAUTICAL AND ASTRONAUTICAL ENGINEERING DEPARTMENT TECHNICAL REPORTS (continued)

Technical Report Number	Title	Author	Journal Publication
AAE 73-10 UILU-ENG 73 0510	Optimal Multiple-Impulse Direct Ascent Fixed-Time Rendezvous	J. E. Prussing L. R. Gross	AIAA J., 12, 885-889 (1974).
AAE 73-11 UILU-ENG 73 0511	The Structure and Stability of Detonation Waves	R. A. Strehlow	
AAE 74-1 UILU-ENG 74 0501	Model of Flame Spreading and Combustion Through Packed Beds of Propellant Grains	H. Krier W. F. Van Tassell S. Rajan J. T. Ver Shaw	BRL Report No. 147 (1974).
AAE 74-2 UILU-ENG 74 0502	On the Nature of Non-Ideal Blast Waves	R. A. Strehlow A. A. Adamczyk	
AAE 74-3 UILU-ENG 74 0503	Viscous Incompressible Flow in Spiral Channels	W. F. VanTassell	
AAE 74-4 UILU-ENG 74 0504	Frequency Response Functions of a Disordered Periodic Beam	J. N. Yang Y. K. Lin	
AAE 74-5 UILU-ENG 74 0505	Predicting Uniform Gun Interior Ballistics: Part I. An Analysis of Closed Bomb Testing	H. Krier S. A. Shimpi	
AAE 74-6 UILU-ENG 74 0506	Predicting Uniform Gun Interior Ballistics: Part II. The Interior Ballistic Code	H. Krier M. J. Adams	
AAE 74-7 UILU-ENG 74 0507	Predicting Uniform Gun Interior Ballistics: Part III. The Concept and Design of the Dynagun Ballistic Simulator	H. Krier J. W. Black	
AAE 74-8 UILU-ENG 74 0508	Process of Fluidization During Porous Solid Propellant Combustion	H. Krier J. T. Ver Shaw	
AAE 74-9 UILU-ENG 74 0509	An Analysis of Flame Propagation Through Coal Dust-Air Mixtures	J. L. Krazinski H. Krier	

RECENT AERONAUTICAL AND ASTRONAUTICAL ENGINEERING DEPARTMENT TECHNICAL REPORTS (continued)

Technical Report Number	Title	Author	Journal Publication
AAE 74-10 UILU-ENG 74 0510	An Interior Ballistics Prediction of the M549 Rocket Assisted Projectile	H. Krier S. Shimpi E. Meister	
AAE 75-1 UILU-ENG 75 0501	Dynamically Induced Thermal Stresses in Composite Material, Structural Panels	A. Zak W. Drysdale	
AAE 75-2 UILU-ENG 75 0502	Numerical Analysis of Laminated, Orthotropic Composite Structures	A. R. Zak	
AAE 75-3 UILU-ENG 75 0503	The Characterization and Evaluation of Accidental Explosions	R. A. Strehlow W. E. Baker	
AAE 75-4 UILU-ENG 75 0504	Program Manual for the Eppler Airfoil Inversion Program	A. I. Ormsbee W. G. Thomson	
AAE 75-5 UILU-ENG 75 0505	Design of High Lift Airfoils with a Stratford Distribution by the Eppler Method	A. I. Ormsbee W. G. Thomson	
AAE 75-6 UILU-ENG 75 0506	Prediction of Flame Spreading and Pressure Wave Propagation in Propellant Beds	H. Krier	
AAE 75-7 UILU-ENG 75 0507	Vigorous Ignition of Granulated Beds by Blast Impact	H. Krier S. Gokhale	